10-25-2023

Evaluation of Equivalent Thermal Conductivity for Carbon Fiber-Reinforced Bentonite through Experimental and Numerical Analysis

Yuan Feng

Jongwan Eun

Seunghee Kim

Yong-Rak Kim

Computers and Geotechnics 165 (2024) 105880

Contents lists available at ScienceDirect

Computers and Geotechnics

journal homepage: www.elsevier.com/locate/compgeo

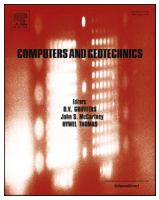

Evaluation of Equivalent Thermal Conductivity for Carbon Fiber-Reinforced Bentonite through Experimental and Numerical Analysis

Yuan Feng [a], Jongwan Eun [a,*], Seunghee Kim [a], Yong-Rak Kim [b]

[a] Civil and Environmental Engineering, University of Nebraska-Lincoln, 1110 South 67th Street, Omaha, NE, USA
[b] Zachry Department of Civil & Environmental Engineering, Texas A&M University, 503H, DLEB, College Station, TX, USA

ARTICLE INFO

Keywords:
Bentonite
Carbon fiber
Thermal conductivity
Analytical solution
FEM

ABSTRACT

Bentonite is widely used as a water-proof material in engineering, and fibers are added to reduce the crack development of bentonite after drying. Carbon fiber can reinforce bentonite in heat-sensitive projects because of its high thermal conductivity and potential inhibition of bentonite cracking. Thus, it is important to determine the thermal conductivity of carbon fiber-reinforced bentonite. This study evaluated the thermal conductivity of carbon fiber-reinforced bentonite by analytical solution, experiment, and finite element method (FEM) simulation and discussed the effects of carbon fiber content, fiber length, fiber distribution, and the porosity of bentonite on the thermal conductivity of reinforced bentonite. The results show that the addition of carbon fiber can effectively improve the thermal conductivity of bentonite, and the thermal conductivity of the mixture is positively correlated with the content of fibers and the dry density of bentonite. When the content of carbon fiber with a thermal conductivity of 1000 W/(m K) is 1.0 %, and the porosity of bentonite is 0.4, the thermal conductivity of the composite can be increased by up to 390 %. At the same time, the distribution of fibers plays a vital role in thermal conductivity, and the thermal conductivity in the case of parallel distribution is 1.48 and 2.91 times that of random distribution and serial distribution. In addition, longer fiber length will help improve the thermal conductivity of the mixture. The thermal conductivity of the mixture for 1-inch fibers is 1.11 and 1.29 times that of 1/2-inch and 1/4-inch fibers. This study provides evidence of the possibility of improving the thermal conductivity of carbon fiber-reinforced bentonite.

1. Introduction

Bentonite is widely used as a barrier material in various engineering applications because of its extremely low hydraulic conductivity in a saturated state (Wersin et al., 2007; Katsumi et al., 2008; Eisenhour et al., 2009; Scalia et al., 2014; Chen et al., 2018; Haynes et al.,2021; Yoon et al., 2022). However, saturated bentonite can crack after drying, significantly reducing its barrier effect. To reduce this cracking, fibers are possibly used to reinforce bentonite. This treatment generates frictional and tensile resistance in the micro-composite between clay particles and the fiber filaments that distribute external forces (Thyagaraj & Soujanya, 2017; Brahmachary & Rokonuzzaman, 2018; Kodicherla & Nandyala, 2019; Bojnourdi et al., 2020). The microfiber filament can also act as a sustained bridge between the particles (Tay et al., 2001; Toé et al.,2006; Zhang et al., 2017; Zhang et al., 2019; Vail et al., 2019; Bekhiti et al., 2019; Liu et al., 2019; Wang et al., 2021, Feng et al., 2021; Guzman & Payano, 2023).

Furthermore, bentonite is required to have proper thermal conductivity in several engineering practices, such as spent fuel repositories and geothermal heating and cooling systems (Delaleux et al., 2012; Wang et al., 2013; Di & Bertermann, 2018; Liu et al., 2019; Lee et al., 2023). For instance, in spent fuel repositories, bentonite is often used as a buffer material, which requires it to control desiccation cracks in high-temperature environments; It also needs to have a high thermal conductivity so that the heat generated by spent fuel can be quickly dissipated into bedrock to prevent core temperatures from exceeding requirements (Beswick et al., 2014; Wang & Hadgu, 2020; Kale et al., 2021; Xu et al., 2022). Also, bentonite is commonly used to fill the space around the pipes in geothermal heating and cooling systems. Using bentonite in geothermal systems helps improve the heat transfer between the pipes and the surrounding soil or water by increasing the contact area and reducing the thermal resistance. Thus, the thermal conductivity of bentonite is very important to control the performance of the applications. However, the thermal characteristics of bentonite

* Corresponding author.
E-mail addresses: yuan91@huskers.unl.edu (Y. Feng), jeun2@unl.edu (J. Eun), seunghee.kim@unl.edu (S. Kim), yong-rak.kim@tamu.edu (Y.-R. Kim).

https://doi.org/10.1016/j.compgeo.2023.105880
Received 18 June 2023; Received in revised form 18 October 2023; Accepted 19 October 2023
Available online 25 October 2023

are subject to its mass density and water content. In general, higher-density materials tend to have higher thermal conductivities. The presence of moisture can significantly affect thermal conductivity, especially in materials with low thermal conductivities in the soils (Allan & Kavanaugh, 1999; Lee et al., 2010; Kim et al., 2015).

Carbon fibers can be used to reinforce bentonite in heat-sensitive engineering due to its high thermal conductivity and potential to inhibit the cracking of bentonite. Carbon fiber-reinforced bentonite is a multiphase mixture that includes air, fibers, water, and bentonite particles. Meanwhile, in the past decades, many studies have been conducted on the equivalent thermal conductivity of multiphase mixed materials (Hamilton & Crosser, 1962; Tong & Zimmerman, 2009; Tarnawski & Leong, 2012; Dong et al., 2015; Likos, W. J. 2015; Zhang & Wang, 2017). These theories consider the effect of a mixture of component content on the equivalent thermal conductivity. Still, most do not consider the fiber's unique geometry, such as the larger aspect ratio of the fiber, which may affect the thermal conductivity of the mixture. Moreover, the distribution of fibers may also affect the equivalent thermal conductivity. For example, the fiber distribution angle is the same as, perpendicular to, or randomly intersects with the heat conduction direction, as shown in Fig. 1 (Shim et al.,2002; Fu & Mai, 2003; Behzad & Sain, 2007; Orakoglu et al., 2016; Liu et al., 2017). However, there is very limited research on using carbon fiber-reinforced bentonite's thermal conductivity associated with various factors, such as carbon fiber content, fiber length, and fiber distribution.

Therefore, this study evaluated the thermal conductivity of carbon fiber-reinforced bentonite through the analytical solution, experiments, and FEM simulations to provide reliable ranges of thermal conductivity for the bentonite mixture. The analytical method was used to analyze the effect of fiber spacing with different fiber content on the equivalent thermal conductivity in the case of a single fiber, considering two cases where the fiber is parallel and perpendicular to the heat conduction direction. Furthermore, the impact of fiber distribution on the equivalent thermal conductivity was discussed by comparing the experimental results with those obtained from FEM simulations. Furthermore, the effects of fiber content, fiber length, fiber distribution, and bentonite porosity on thermal conductivity were evaluated by using the FEM simulation.

2. Thermal Conductivity of Composite Materials

2.1. Theoretical models

2.1.1. Wiener model

Wiener (1912) noted that the thermal conductivity of porous media has upper and lower limits depending on the distribution of the various components, including solids, gases, and liquids. The equivalent thermal conductivity will reach the upper bound when all components are arranged in parallel, as shown in Fig. 2(a), and it can reach the lower bound when all components are arranged in series, as shown in Fig. 2(b). The equivalent thermal conductivities of mixtures arranged in parallel and series connections can be expressed respectively as:

$$\lambda_W^U = \sum \phi_\alpha \lambda_\alpha (parallel) \tag{1a}$$

$$\lambda_W^L = \left[\sum \frac{\phi_\alpha}{\lambda_\alpha} \right]^{-1} (serial) \tag{1b}$$

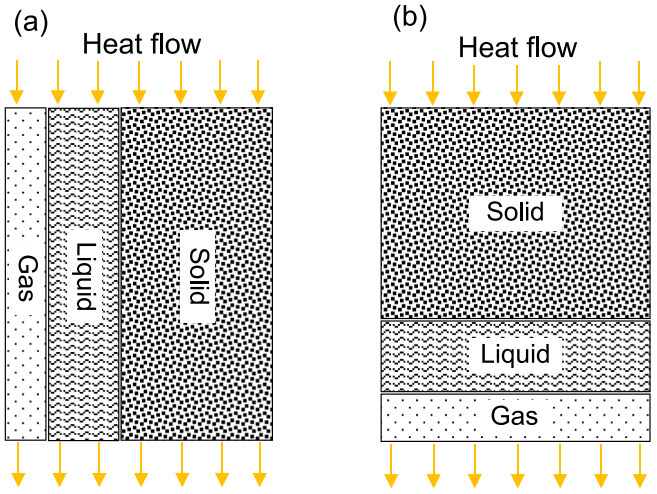

Fig. 2. Schematic diagram of Wiener bounds of porous media, (a) Parallel connection; (b) Serial connection.

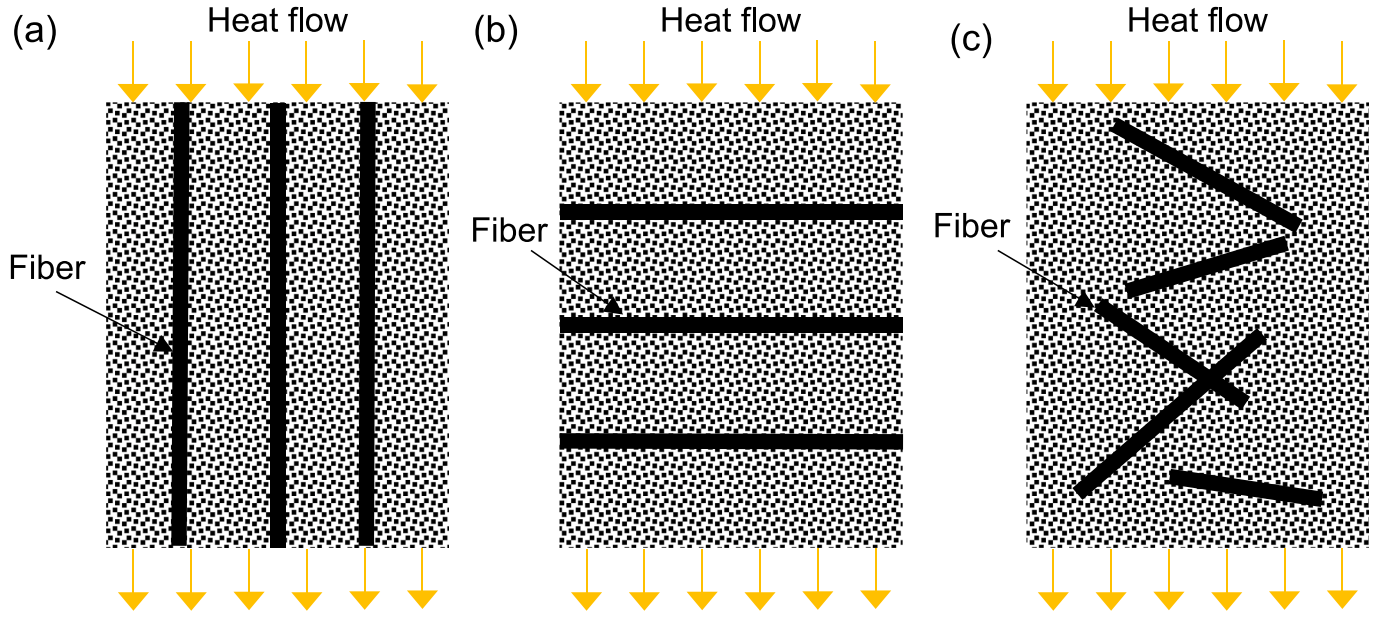

Fig. 1. Schematic diagram of heat transport through fiber-reinforced bentonite under different fiber orientation conditions. (a) serial, (b) parallel, (c) random.

where ϕ_α and λ_α are the volume fraction and thermal conductivity (W/(m·K)) of the α phase, respectively. These two bounding limits are the so-called Wiener bounds, and the independent of pore structure. Eqs. (1a) and 1b) correspond to the upper and lower Wiener bounds and are expressed by λ_W^U and λ_W^L (W/(m·K)), respectively.

2.1.2. Hashin–Shtrikman model

For isotropic mixtures, the equivalent thermal conductivity bounds are independent of the pore structure, the thermal conductivities of (N + 1)-isotropic phases of the isotropic mixture can be denoted as and their volume fractions as $\phi_0,\phi_1,\cdots,\phi_N \in [0,1]$, respectively (Phan-Thien & Milton, 1982; Carson et al., 2005; Zimmerman 1989; Liu 2007). Here, $0 < \lambda_0 < \lambda_1 < \cdots < \lambda_{N-1} < \lambda_N$. The lower and upper bounds of Hashin–Shtrikman (H-S) model can then be expressed as,

$$\lambda_{H-S}^L = \lambda_0 + \frac{n\lambda_0 \sum_{i=1}^{N} \phi_i/(1+c_i^L)}{\phi_0 + \sum_{i=1}^{N} \phi_i c_i^L/(1+c_i^L)} \tag{2a}$$

$$\lambda_{H-S}^U = \lambda_N + \frac{n\lambda_N \sum_{i=0}^{N-1} \phi_i/(1+c_i^U)}{\phi_N + \sum_{i=0}^{N-1} \phi_i c_i^L/(1+cU)} \tag{2b}$$

where,$c_i^L = n\lambda_0/(\lambda_i - \lambda_0)$ and $c_i^U = n\lambda_N/(\lambda_i - \lambda_N)$, n is the number of dimensions, either 2 or 3.

2.2. Fiber soil composite

Most models to predict soil thermal conductivity do not consider the influence of component geometry or treat fiber as spherical particles, such as the above-mentioned Wiener model and H-S model (Pietrak and Wiśniewski, 2015; Zhang et al., 2017). However, the geometry of components plays a significant role in determining the thermal conductivity of fiber-reinforced soils, especially fibers with higher conductivity, as fibers have a large aspect ratio (Wang et al., 2007, 2009). The models treat fiber as spherical, underestimating the enhancement effect (Pietrak and Wiśniewski, 2015). Not only is it difficult to accurately predict the thermal conductivity of fiber-reinforced soils due to the geometry of the fibers, but the geometry will cause heat conduction to occur in certain directions in the mixture. Some studies have proposed models to predict the thermal conductivity of fiber composite, which consider factors such as fiber aspect ratio, bending, and interface thermal resistance (Deng et al., 2007; Liu et al., 2017; Burger et al., 2016; Macias et al., 2019). However, these models still deviate from the experimental results because of the randomness of fiber distribution. Numerical simulation is a method to predict the thermal conductivity of mixtures, which can include a description of the fiber distribution and structural characteristics (Yang et al., 2015; Chen et al., 2016). For example, a uniform random distribution of fibers or a specific distribution due to the manufacturing process of the fiber composite can be reflected in the model. Many studies have used the random fiber distribution model generated by automatic algorithms to evaluate the mechanical properties of fiber composite, considering fiber content, aspect ratio, distribution, contact conditions, etc. (Lu et al., 2015; Sun et al., 2019; Gao et al., 2021). Some researchers have also applied this model to the thermal conductivity analysis of fiber composite (Zhai et al., 2018).

3. Estimation of Thermal Conductivity for Fiber-Reinforced Bentonite

3.1. Analytical solution of single fiber case

A single fiber case was considered to evaluate the effect of fiber geometry and distribution on the equivalent thermal conductivity. The fiber had a dimension of 12.7 mm in length and 0.01 mm in diameter. Parallel and series cases were discussed for different directions of heat conduction. Three different fiber contents were discussed, which were 0.5 %, 1.0 %, and 2.0 % by gravity. The thermal conductivity of carbon fiber and saturated bentonite used in the single fiber case evaluation was 1000 W/(m·K) and 1.59 W/(m·K), respectively.

Fiber-reinforced bentonite comprises bentonite particles, fibers, liquid water, and air. The air in the mixture is negligible at the fully saturated condition. However, when not saturated, the voids are filled with air, which causes the heat transfer phenomenon to behave differently. When heat flows through the interface between the composite components, a temperature drop occurs at the interface. Sundberg (1988) introduced a dimensionless heat transfer correction coefficient to represent the reduction of heat flow due to imperfect contact between grains. Tarnawski et al., (2002) indicated that the heat transfer correction coefficient is limited for saturated soil. The voids between the bentonite particles and fibers are filled with water, and water bridges are formed between soil particles and fibers (Ewing and Horton, 2007; Lu et al., 2014). We assumed perfect thermal conduction at the interface between the fibers and water or bentonite particles and water, i.e., having the same temperature.

To calculate the equivalent thermal conductivity of the fiber-bentonite mixture in the single fiber case, the idealized geometry of the mixture can be seen as series and parallel combinations of bentonite and fibers, as shown in Fig. 3. The mixture was divided into five blocks: parts 1 to 4 were saturated bentonite and part 5 was fiber. For the parallel case, heat transport was from right to left. Firstly, the equivalent thermal conductivity λ_{1_p} of blocks 1, 2, and 5 connected in parallel was calculated, as shown in Eq. (3a). Then, the blocks connected in the first step were connected with blocks 3 and 4 in series to get the overall equivalent thermal conductivity λ_{equiv}, which can be expressed as:

$$\lambda_{1\_p} = \frac{H-D}{H}\lambda_{b\_s} + \frac{D}{H}\lambda_f \tag{3a}$$

$$\lambda_{equiv} = \frac{L}{l/\lambda_{1\_p} + (L-l)/\lambda_{b\_s}} \tag{3b}$$

where D and l are the diameter and length of carbon fiber (m), respectively; L and H are the length and thickness of the fiber-bentonite

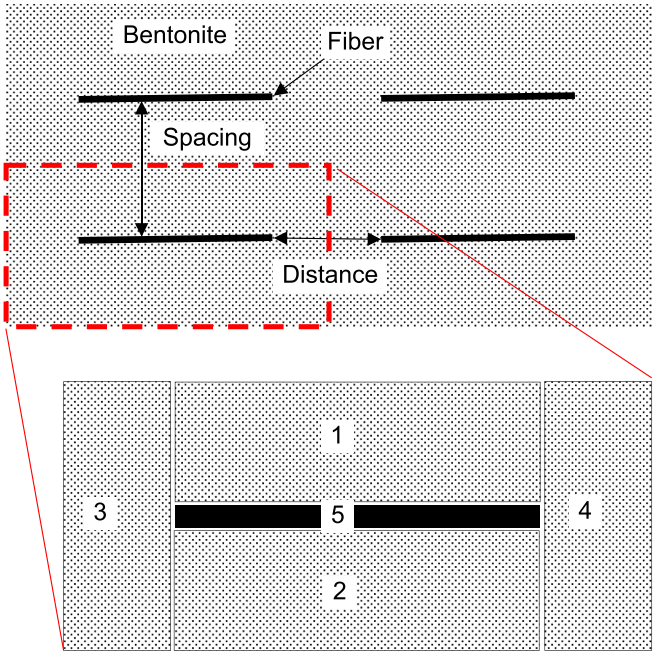

Fig. 3. Schematic diagram of heat transport through fiber-reinforced bentonite, single fiber case. The 'Distance' is the length between the vertices of the nearest two fibers, the 'Spacing' is the distance between two parallel fibers.

mixture (m), respectively; λ_f and λ_{b_s} are the thermal conductivity of carbon fiber and saturated bentonite (W/(m·K)), respectively.

For the serial case, heat transport from top to bottom. Firstly, we calculate the equivalent thermal conductivity λ_{1_s} of 1, 2, and 5 blocks connected in series; and then connect the blocks connected in the first step with 3 and 4 blocks in parallel to get the overall equivalent thermal conductivity λ_{equiv}, which can be expressed as,

$$\lambda_{1\_s} = \frac{H}{D/\lambda_f + (H-D)/\lambda_{b\_s}} \tag{4a}$$

$$\lambda_{equiv} = \frac{l}{L}\lambda_{1\_s} + \frac{L-l}{L}\lambda_{b\_s} \tag{4b}$$

3.2. Experimental

3.2.1. Material: carbon fiber and bentonite

The commercially available carbon fibers (produced by HYOSUNG Advanced Materials, South Korea) with circular cross-sections are used in this study, and the length of the chopped fiber is 12.7 mm (1/2 in.). The diameter of the carbon fibers is 7.0 μm to 10.0 μm.

The sodium bentonite used in this study is a commercial one produced from natural bentonite in Wyoming, USA (Sturgis Materials, Kansas City). The bentonite particles are granular, mostly ranging from 0.5 mm to 2.0 mm. The grain size distribution is shown in Fig. 4. It has a plastic limit of 95 %, a liquid limit of 400 %, and a specific gravity of 2.69. Sodium bentonite contains more than 80 % montmorillonite and other minerals such as quartz, plagioclases, carbonates, mica, and K-feldspars (Montes-H & Geraud, 2004). Those properties are listed in Table 1.

Table 1
Physical properties of bentonite used in this study.

Soil properties	Values
Specific gravity	2.69 [1]
Bulk density	1.03 g/cm^3
Swell index	32 mL/2g [2]
Liquid limit	400 %
Plastic limit	95 %
Plasticity index	305

[1] Ravi and Rao (2013)
[2] Scalia et al (2018)

3.2.2. Sample preparation

The cylindrical samples with a diameter of 101.6 mm and a height of 42.5 mm were used for the experiment. For two samples, the porosity was 0.4 or 0.6, and the dry density was 1.61 or 1.08 g/cm3 after saturation. The fiber content is 1.0 % by weight. The samples were prepared by mixing oven-dried bentonite with fibers and water and then compacting them layer by layer until they were saturated. First, the dried granular bentonite was gradually mixed with adding water using a blender. Once the required moisture content was reached, the carbon fibers were added and mixed until the distribution of the fibers did not change. After mixing with the blender, there were still clusters of fibers, so the large fiber clusters were carefully broken into smaller ones by hand. Then, the fiber-bentonite mixture was placed in a sealed bag for 24 h. Finally, the mixture was compacted layer by layer with a hammer in the compaction mold and compressed with a hydraulic jack to ensure that the mixture reached a saturated state. Fig. 5(b) shows the prepared sample. Since the sample is compacted layer by layer, the distribution of fibers tends to be randomly distributed in a plane parallel to the horizontal plane, as shown in Fig. 5(c) and 5(d).

3.2.3. Measurement of thermal conductivity

A dual probe sensor (SH-3 sensor produced by METER GROUP) was used in this study, which is widely used in the thermal conductivity measurement of bentonite and other soil (Abu-Hamdeh, 2001; Zhang et al., 2015; Nikoosokhan et al., 2016; Xu et al., 2019; Yoon et al., 2019). The sensor has two steel needles with a length of 30 mm and a diameter of 1.3 mm with a spacing of 6 mm, as shown in Fig. 5(a). The two needles are the heat source and temperature sensor, respectively. The sensor can obtain thermal conductivity and heat capacity, with a measurement range of 0.02——2.0 W/(m·K) and 0.5——4.2 MJ/(m^3·K), respectively. The principle and process of the sensor measuring thermal conductivity are as follows (Bristow et al., 1994): The heat source needle releases heat for a certain period and then turns it off. The temperature sensor needle measures the temperature change when the heat source needle releases heat. The temperature sensor continues to measure the temperature until the measured temperature reaches the maximum value and stops the temperature measurement. The testing data in this study was collected using the KEYSIGHT DAQ970A data acquisition system. Fig. 6 shows the temperature versus time curves while measuring the thermal conductivity of sensor calibration standard and carbon fiber-reinforced

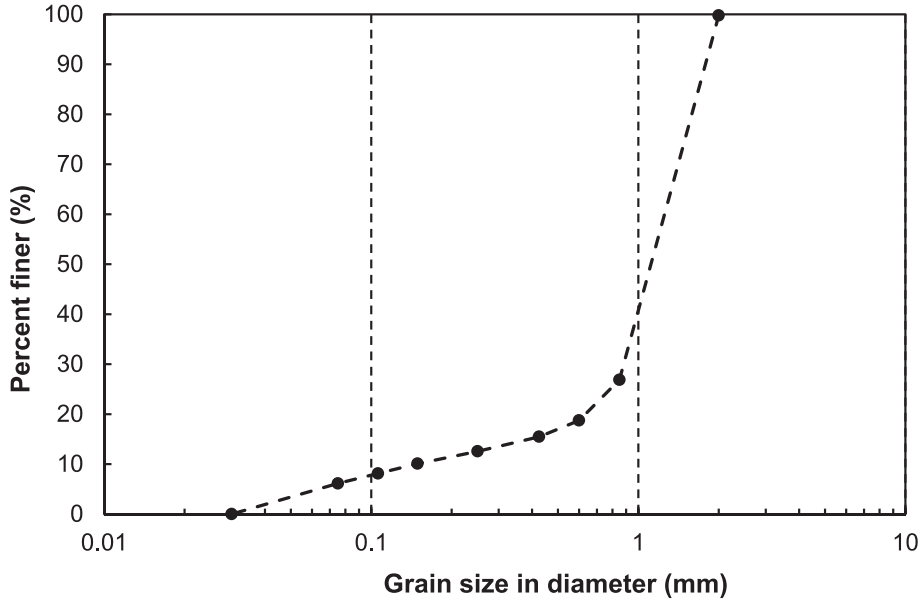

Fig. 4. The grain size distribution of the sodium bentonite used in this study.

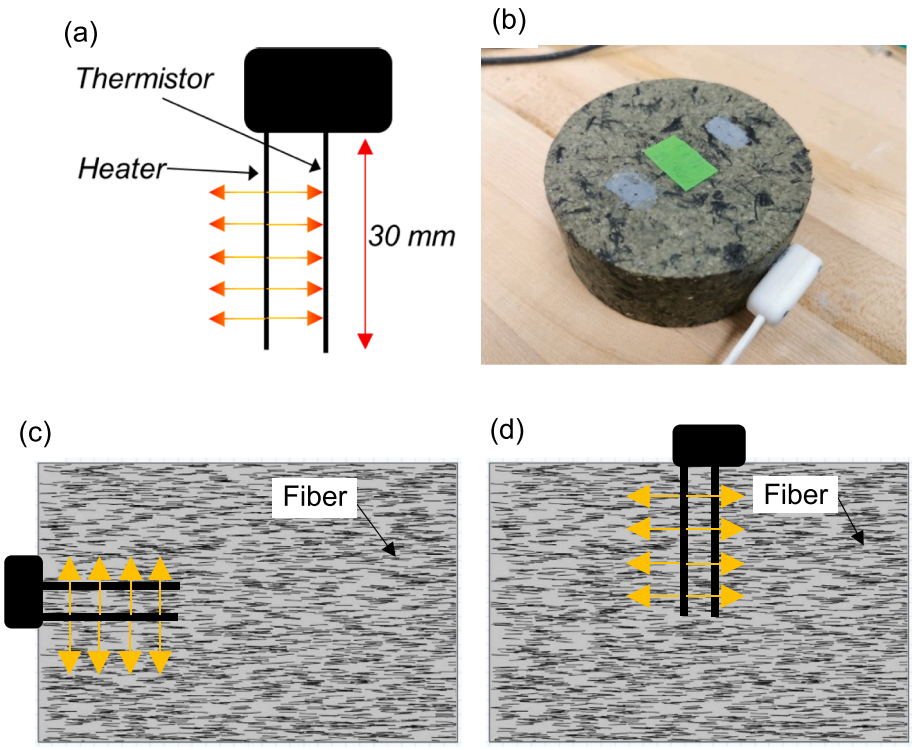

Fig. 5. Measurement of the thermal conductivity of the carbon fiber-reinforced bentonite. (a) Schematic of the dual needle sensor; (b) measurement photo, sample with the size D: 101.6 mm; H: 42.5 mm; (c) sensor installation direction – horizontal; (d) sensor installation direction – vertical.

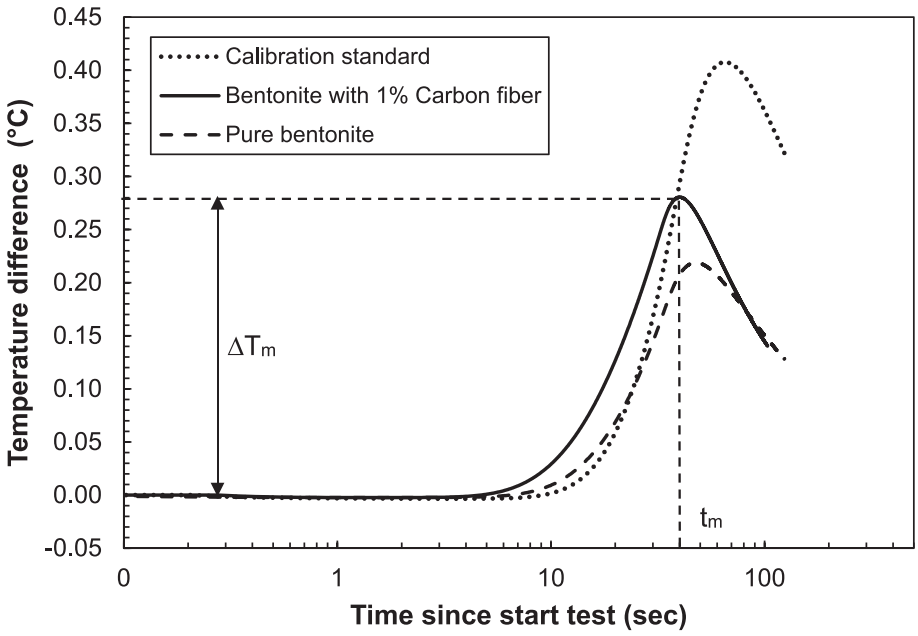

Fig. 6. Comparison of the thermal conductivity test data of calibration standard, bentonite with 1.0% carbon fiber, and pure bentonite.

bentonite. The data was processed by following equations,

$$\lambda = D * C_p \tag{5a}$$

$$D = \frac{r^2}{4}\left\{\frac{(t_m - t_0)^{-1} - t_m^{-1}}{\ln[t_m/(t_m - t_0)]}\right\} \tag{5b}$$

$$C_p = \frac{q}{4\pi D \Delta T_m}\left\{Ei\left[\frac{-r^2}{4D(t_m - t_0)}\right] - Ei\left[\frac{-r^2}{4Dt_m}\right]\right\} \tag{5c}$$

where λ is the thermal conductivity (W/m•s); D is the thermal diffusivity (m2/s); C_p is the heat capacity (J/m^3·K); r is the needle spacing (m); t_m is the time reaches the maximum temperature (s); t_0 is the heating time (s); q is the heat input at the heater needle (W/m); ΔT_m is the maximum temperature difference at thermistor needle (K); Ei is the exponential integral.

To measure the anisotropy of thermal conductivity caused by fiber distribution, the thermal conductivity of carbon fiber-reinforced bentonite was measured from two directions. The sensor installation is

shown in Fig. 4(c) and 4(d), parallel and perpendicular to the horizontal plane, respectively.

3.3. Numerical Simulation

3.3.1. Thermal conduction

Thermal conduction (or diffusion) results from different mechanisms in different media. Theoretically, in the air it occurs in the gas through molecular collisions. In a continuum, Fourier's law of heat conduction states that the conduction heat flux, q, is proportional to the temperature gradient,

$$q = -k\nabla T \tag{6}$$

where k is the thermal conductivity (W/(m·K)). The heat transfer in a solid can be expressed as,

$$\rho C_p \frac{\partial T}{\partial t} + \nabla q = 0 \tag{7}$$

where ρ is the density of materials (kg/m^3)

3.3.2. Numerical modeling

A series of two-dimensional (2D) thermal conduction cases were conducted using a FEM to evaluate the thermal conductivity of carbon fiber-reinforced bentonite. The commercial software COMSOL Multiphysics was used to perform the simulation. To evaluate the effect of the fiber distribution on the thermal conductivity of the fiber-bentonite mixture, randomly distributed fibers were constructed in the computational model. The coordinates of two points controlled each fiber's position, direction, and length. The fibers with different distribution directions were generated by controlling the angle between the fiber and the horizontal direction, as shown in Fig. 7(a). The coordinates of the two vertices of a single fiber with a length of L were (x_1, y_1) and (x_2, y_2), respectively. The angle between the fiber and the horizontal direction was θ. The coordinates of random fibers were generated by MATLAB. Fig. 7(b) shows the bentonite mixture model of randomly distributed fibers when the fiber length is 12.7 mm and the fiber content is 1.0 % by gravity, where the inclination angle and position of each fiber in the area are randomly distributed. The number of fibers in the model domain varies according to fiber content, diameter, length, and model size. The number of fibers in the domain can be calculated as,

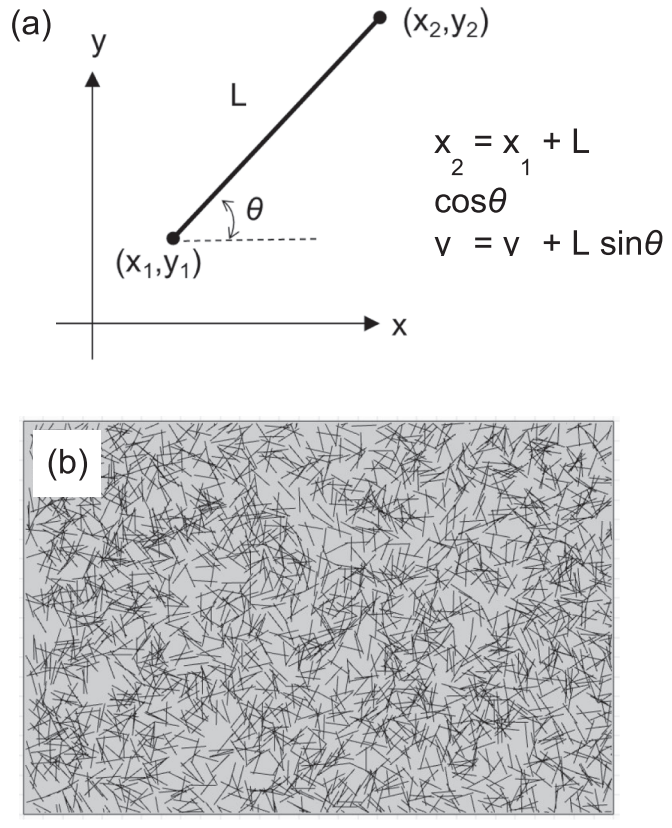

Fig. 7. Schematic diagram of the randomly distributed fiber-reinforced bentonite. (a) single fiber, (b) randomly distributed fiber model.

$$N_f = \frac{\phi_f A_m}{dl} \tag{8}$$

where N_f is the number of fibers; ϕ_f is the volume fraction of fibers; A_m is the model domain area (m^2); d and is the diameter and length of fibers (m), respectively.

3.3.3. Model parameterization

The thermal conductivity of carbon fiber-reinforced bentonite was simulated when bentonite was saturated. The simulation considered a variety of parameters, including fiber content, fiber length, porosity, bentonite dry density, and fiber distribution orientation, as listed in Table 2. The simulation considered bentonite porosities of 0.2, 0.4, and 0.6, and the corresponding dry densities were 2.15 g/cm^3, 1.61 g/cm^3, and 1.08 g/cm^3, respectively. The laboratory measurement was compared with simulations of carbon fibers with a thermal conductivity of 200 W/(m·K). In addition, carbon fibers with a thermal conductivity of 1000 W/(m·K) were used to analyze the thermal conductivity of the fiber-bentonite mixture due to various factors. The saturated bentonites used in this simulation have thermal conductivity values of 1.89 W/(m·K), 1.59 W/(m·K), and 1.31 W/(m·K) from measurement, corresponding to porosities of 0.2, 0.4, and 0.6, respectively.

The size of the model in the simulation is 0.3 m × 0.2 m. Fig. 8 shows the models for random ($-90° < \theta < 90°$), parallel ($-5° < \theta < 5°$), and serial ($85° < \theta < 90°$, $-90° < \theta < -85°$) fiber distribution with a fiber content of 1.0 % by gravity. The length of the fibers is 12.7 mm. In the simulation, the temperatures on the left and right sides of the model are 20 °C and 50 °C respectively; the upper and lower boundaries are no heat flow, and the heat diffuses from the right side to the left side of the fiber-bentonite mixture. The thin layer element with a thickness of the diameter of carbon fiber represents the fibers in the simulation. As a perfect contact between saturated bentonite and carbon fiber is assumed, the bentonite and fiber have the same temperature at the contact interface. Overlapping fibers are considered as a unit. At the same time, the mesh near the fibers is refined, as shown in Fig. 8(a). For example, the model mesh corresponding to Fig. 8(a) has 696,643 triangular meshes and 77,565 edge meshes.

Meanwhile, the equivalent thermal conductivity in the case of the single fiber case mentioned in Section 2.2 was also analyzed by simulation. Similar to the mixture, the fiber in the simulation has a length of

Table 2
Simulation cases.

Fiber thermal conductivity (W/m K)	Fiber distribution	Fiber content (%)	Fiber length (Inch)	Comments
200	Random/ Parallel/ Serial	1.0	0.5	Compared with experiment
1000	Parallel/ Serial	0.5/1.0/ 2.0	0.5	Single fiber case
1000	Random	0.5/1.0/ 2.0	0.25/ 0.5/1.0	
	Parallel	0.5/1.0/ 2.0	0.25/ 0.5/1.0	
	Serial	0.5/1.0/ 2.0	0.25/ 0.5/1.0	

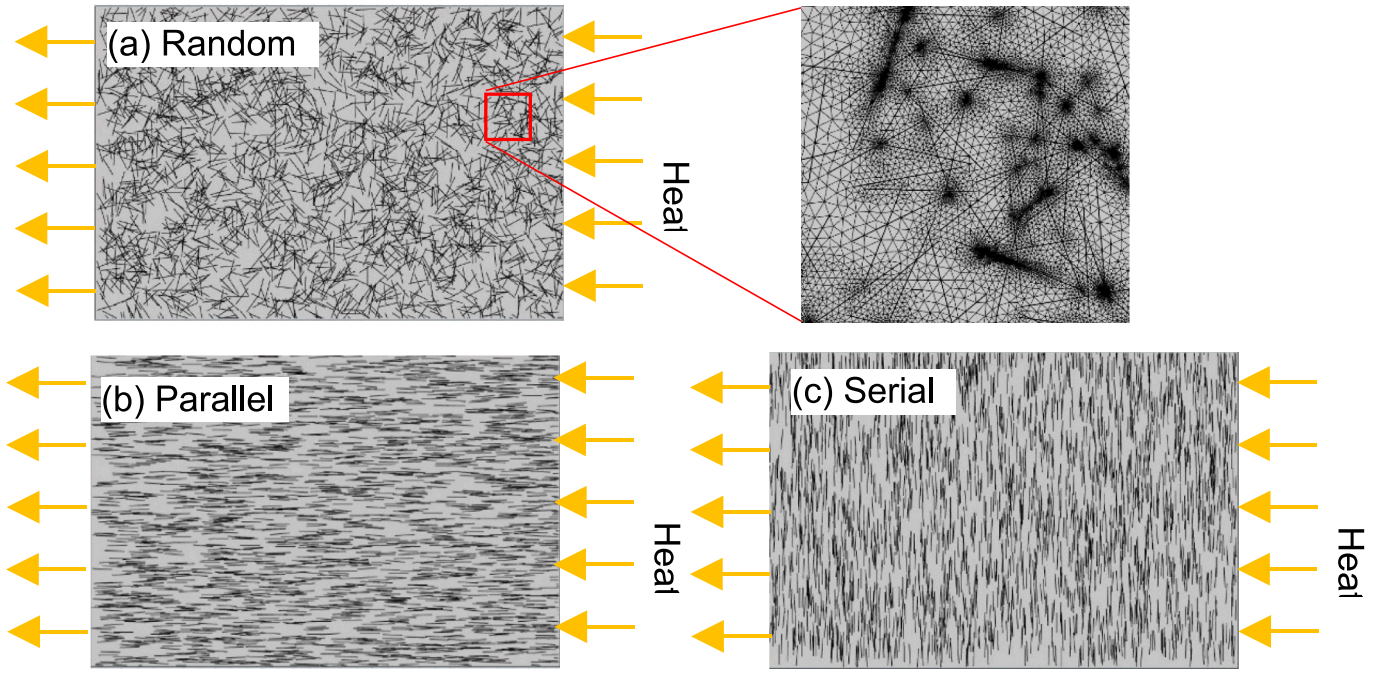

Fig. 8. Simulation cases of heat transport through fiber-reinforced bentonite under different fiber orientations. (a) random ($-90° < \theta < 90°$) fiber distribution model and mesh of fiber filament, (b) parallel ($-5° < \theta < 5°$) fiber distribution, (c) serial ($85° < \theta < 90°$, $-90° < \theta < -85°$) fiber distribution.

12.7 mm and a diameter of 0.01 mm. Both parallel cases and serial cases are evaluated.

4. Results and Discussions

4.1. Single fiber case

When carbon fiber reinforced bentonite is used in engineering applications, it is necessary to consider the direction of heat conduction due to the different temperature conduction with the boundaries or with the direction of the fiber additives in the mixture. For example, when used as a buffer material in spent fuel repositories, there is a higher temperature near the canister and a lower temperature near the host rock. Accordingly, the engineered barrier shows the overall heat transfer from a higher temperature boundary to a lower temperature boundary. Moreover, since the distribution direction of fibers can be controlled by layer-by-layer compaction during material preparation, there are different angles between the orientation of fibers and the direction of heat conduction. Thus, the buffer material at different locations has different heat conduction directions, such as around the canister or under and above the canister (Finsterle et al., 2019; Levasseur et al., 2022).

For the single fiber case, the volume of bentonite is fixed for a specific fiber content. The distance between fibers becomes smaller when the spacing increases, as shown in Fig. 3. The fibers would be connected when the spacing increases to the maximum. Fig. 9 shows the analytical solution and simulation results of equivalent thermal conductivity for carbon fiber-reinforced bentonite in the case of a single fiber. The analytical solution and simulation results are in good agreement. As for the parallel case, the equivalent thermal conductivity of the fiber-bentonite mixture increases as the increase of spacing between the fibers, as shown in Fig. 9(a). The equivalent thermal conductivity increases from 1.61 W/m K to 3.54 W/(m·K), 5.55 W/(m·K), and 9.48 W/(m·K) with fiber spacing increase at the fiber content of 0.5 %, 1.0 %, and 2.0 %, respectively. The distance decreases to 0 when the spacing increases to the maximum, which means that the fibers are connected to each other, and the thermal conductivity reaches the maximum value in this case. The direction of heat conduction is the same as the extension direction of the fiber, and the presence of fibers dramatically enhances heat conduction.

On the other hand, the fibers are piled together when the spacing decreases to 0, and the thermal conductivity decreases to a minimum. For the serial case, the equivalent thermal conductivity increases by a negligible value as the decreased spacing. This is because the fiber extension direction is perpendicular to the heat conduction direction, the fibers are isolated by bentonite, and the thermal conduction mainly occurs in bentonite.

It follows from the above that the parallel distribution is significantly beneficial for improving the thermal conductivity compared to the series distribution due to the special shape characteristics of the fibers. The aspect ratio of particles significantly affects the equivalent thermal conductivity of anisotropic multi-phase materials. A smaller aspect ratio of particles gives a higher thermal conductivity of the composite in the major axes' direction (Akbari et al., 2013). For the carbon fibers used in this study, the aspect ratio of a 12.7 mm long fiber is 1270, which means that the thermal conductivity of the fiber-bentonite mixture is significantly higher in the direction of fiber orientation than in the direction perpendicular to the fiber orientation. If the fiber length is longer, the equivalent thermal conductivity in the direction of fiber orientation will be greater.

4.2. Comparison of theoretical models, experimental, and FEM simulation

The above-mentioned single fiber case shows the difference in equivalent thermal conductivity caused by the fiber distribution. In contrast, many fibers mixed with bentonite will lead to a more complex fiber distribution and different equivalent thermal conductivity than the single fiber case. Fig. 10 shows the comparison of the equivalent thermal conductivity obtained from theoretical bounds, experimental measurement, and FEM simulation results in the case of the thermal conductivity of carbon fiber equal to 200 W/(m·K) and the fiber with a length of 12.7 mm (1/2 in.). In the experiment, two samples with different dry densities were prepared, and triplicate sets of thermal conductivity measurements in two directions were carried out. There was no significant difference in the thermal conductivity of each sample in the two directions. Here, the average value of the measurement results of each

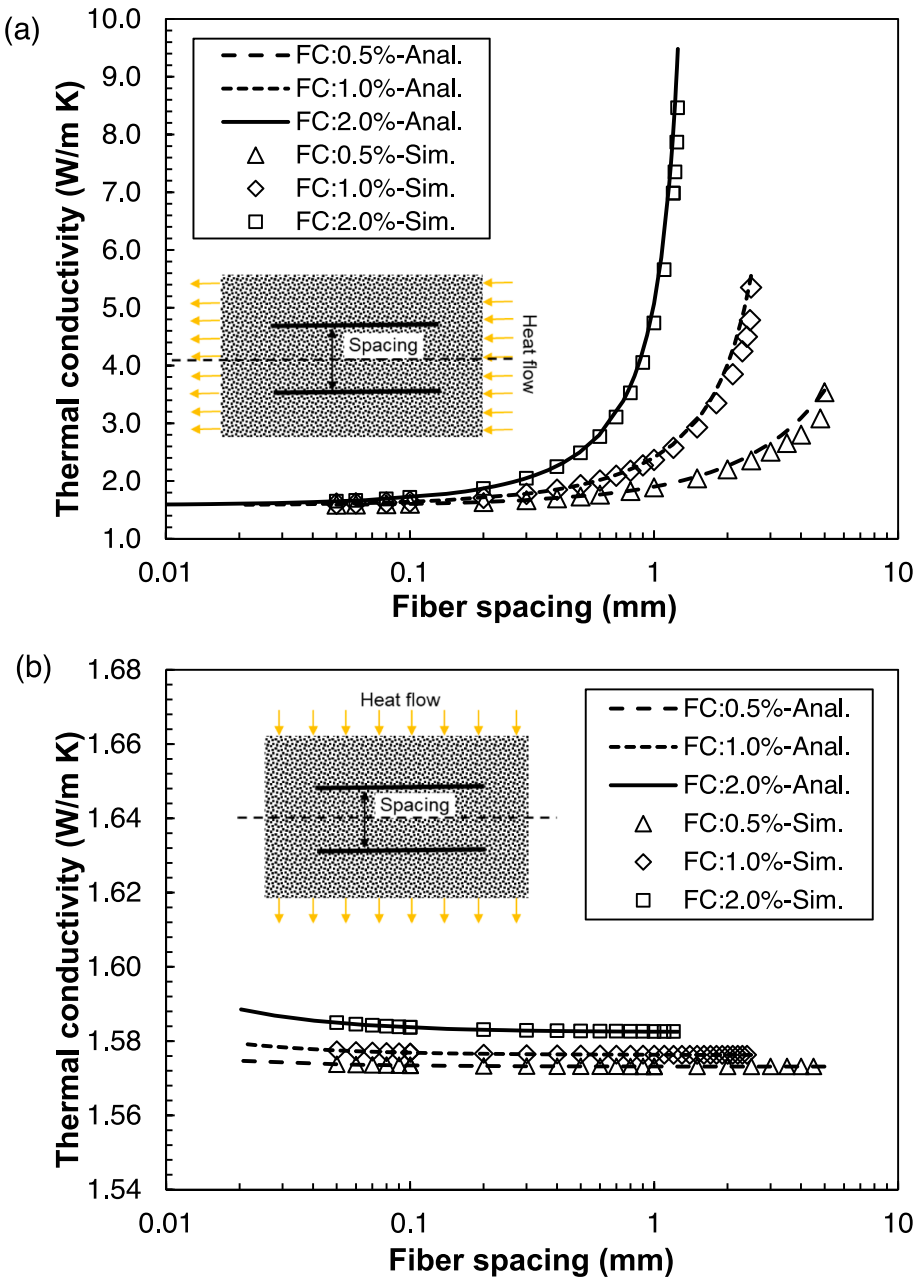

Fig. 9. Comparison of thermal conductivity in the case of single fiber for carbon fiber reinforced bentonite by analytical solution and simulation, fiber length is 0.5 in.; fiber contents are 0.5%, 1.0%, and 2.0% by gravity; (a) parallel, (b) serial.

sample is shown in Fig. 10, the standard deviation of samples with dry densities of 1.61 and 1.08 g/cm^3 are 0.04 and 0.09, respectively. Wiener bounds have a wider range of estimates than H-S bounds for equivalent thermal conductivity. For isotropic porous media, the equivalent thermal conductivity should fall within the H-S bounds. For the case where the fiber length is 0.5 in., the distribution of the position of fibers is random. The fiber-reinforced bentonite can be regarded as approximately isotropic, so the equivalent thermal conductivity of the mixture falls within the H-S bounds. However, due to the special geometry of carbon fibers, the heat transfer in fiber-reinforced bentonite gives different equivalent thermal conductivity according to different fiber distributions.

For the simulation, the equivalent thermal conductivity for the parallel cases and serial cases in terms of the fiber distribution is close to the upper and lower bound of H-S bounds, respectively. The random cases of the fiber distribution fall within the middle. This result agrees with the evaluation in a single fiber case that parallel distribution would have a higher equivalent thermal conductivity. In the parallel cases, the orientation of the fibers with a small angle with heat flux direction, and the carbon fiber with higher thermal conductivity and elongated geometry facilitate the heat transport. However, in the serial cases, the fibers are isolated by the bentonite in the direction of the heat flux direction and bentonite dominates the thermal conductivity. The equivalent thermal conductivity is close to the value of bentonite. The equivalent thermal conductivity changes with the angle change between the direction of fiber orientation and the heat conduction direction (Wang et al., 2007, 2009). When the fiber distribution is between a random distribution and parallel distribution, that is, the angle between the direction of fiber orientation and the heat conduction direction is $-45^\circ < \theta < 45^\circ$, the equivalent thermal conductivity is also between the two distribution situations.

The experimental results are close to the lower bound of the H-S

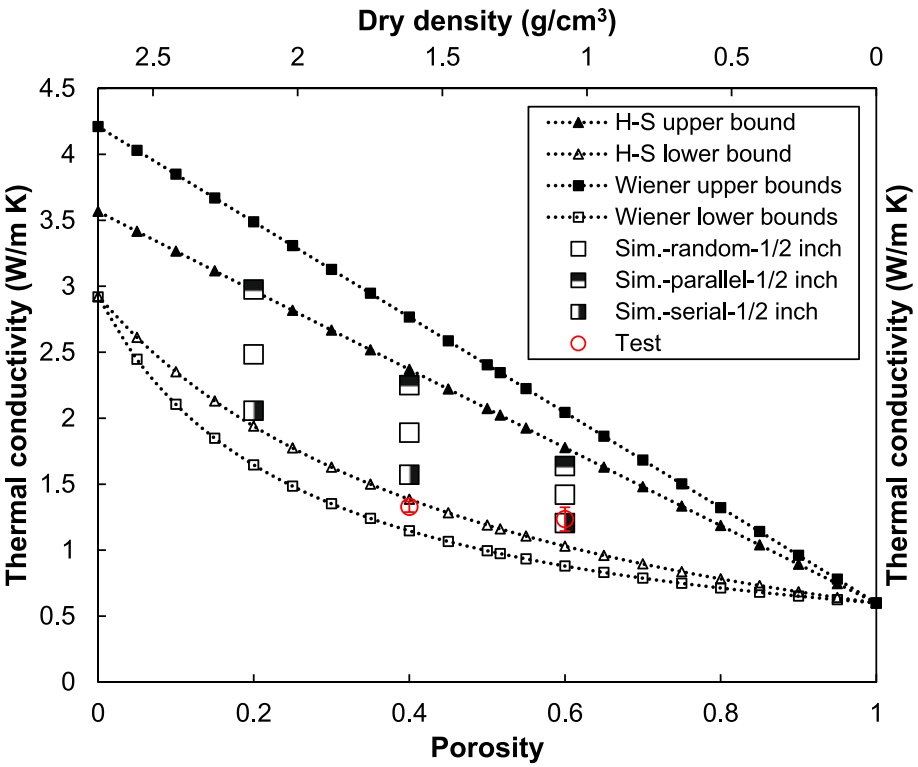

Fig. 10. Comparison of the thermal conductivity for H-S bounds, Wiener bounds, experimental result, and FEM simulation result; fiber distribution orientations are random, parallel, and serial; fiber length is 0.5 in.; fiber content is 1 % by gravity; carbon fiber thermal conductivity is 200 W/(m K).

bound and the simulation results for the series case because the distribution of fibers in the sample is closer to the series case. It is difficult to ensure the uniform distribution of fibers in the process of preparing samples. The compaction of the mixture, along with layer-by-layer, brings the extension angle of fibers close to the horizontal direction. Also, the fibers in the simulation model are straight, while the fibers in the experiment are bent and distributed in clusters. Straight and evenly distributed fibers are conducive to forming fiber networks to improve the equivalent thermal conductivity, while the fiber distribution in the experiment is not conducive to heat conduction (Liu et al., 2017). In addition, the thermal contact resistance between fibers and bentonite is also a possible reason for reducing the function of the carbon fiber, even though the samples were compacted layer by layer. The compacted mixture is almost completely saturated, but some voids may still be filled with air at the fiber and bentonite interface. Air has an extremely low thermal conductivity compared to water, greatly increasing interfacial thermal resistance (Dong et al., 2015; Wen et al., 2022a). The air between the fibers and the bentonite particles may reduce the enhancement effect of carbon fibers.

Moreover, the clusters and bending of fibers, as shown in Fig. 5(b) on the surface of the sample, make it a challenge to play the role of fibers in promoting the equivalent thermal conductivity. Clusters of fibers affect the equivalent thermal conductivity, Wang et al. (2016a, 2016b) proposed that the equivalent thermal conductivity is related to the degree of clustering and the clustered arrangement of fibers. The clustered fiber distribution may inhibit the heat flux, which requires us to propose a mixing method to improve the uniform distribution of fibers in practical applications (Javanbakht et al., 2019). The cluster distribution of fibers is not conducive to increased thermal conductivity (Wang et al., 2016a, 2016b). When the fiber content is fixed, the number of fibers in a cluster of fibers affects the number of fiber clusters. The number of fiber clusters significantly affects the formation of fiber networks. If most of the fibers are distributed as clusters, it is difficult to form a fiber network. The formation of fiber clusters reduces the possibility of network formation to connect the heat transfer channel through the bentonite, which is more important for heat conduction. More fiber clusters will form a weaker network, which is not conducive to the role of fibers. In the case of serial, carbon fiber has little effect on improving the equivalent thermal conductivity overall, and the effect of fiber clusters can be ignored. In the case of parallel, the existence of fiber clusters may significantly affect the overall thermal conductivity, and it is worth considering ensuring the uniform distribution of fibers in the preparation of mixtures for practical engineering applications. Since the actual morphology of microfibers in the mixture is difficult to obtain and describe, there are few systematic studies on the effect of fiber bending on the equivalent thermal conductivity of fiber mixtures. When the carbon fiber distribution direction is consistent with the heat conduction direction is most conducive to heat conduction, but the bending of fibers may reduce the enhancement effect. The relationship between the degree of bending and the efficiency of heat conduction deserves more research, which can help to adopt a more effective mixing method in practical applications.

Meanwhile, the equivalent thermal conductivity of carbon fiber-reinforced bentonite increases with the increase of the dry density. Carbon fiber-reinforced bentonite used in this study is a mixture of water, bentonite, and carbon fiber in a saturated state. As the dry density increases, the proportion of bentonite particles increases, and the volume content of fibers increases as well. More fibers lead to higher equivalent thermal conductivity. Even in the case of serial cases, a higher proportion of bentonite particles can lead to a higher equivalent thermal conductivity due to its higher thermal conductivity than water.

4.3. *Effect of fiber length, distribution, and content*

Depending on the various thermal conductivity of carbon fiber, the thermal conductivity of the fiber-bentonite mixture can vary significantly. The thermal conductivity of carbon fiber manufactured based on new technology can be higher than 1000 W/(m·K). For example, the

carbon fiber produced by Nippon Graphite Fiber Corporation has a thermal conductivity of 1200 W/(m·K). Some carbon fibers based on carbon nanotube technology can have a thermal conductivity higher than 3000 W/(m·K) (Fujii et al., 2005; Kumanek & Janas, 2019). When the fiber thermal conductivity is higher, the composite thermal conductivity increases significantly with the fiber length, fiber content, and fiber distribution (Fu et al., 2003). Bentonite reinforced with those carbon fibers may have better heat-conducting properties. Fig. 11 shows the comparison of the equivalent thermal conductivity for theoretical bounds, and the FEM simulation result in the case of the thermal conductivity of carbon fiber is 1000 W/(m·K). Fig. 11(a) to (c) show the comparison of the fiber distribution of random, parallel, and serial cases, respectively. Similar to the cases of carbon fiber with a thermal conductivity of 200 W/(m·K), parallel cases have a higher equivalent thermal conductivity than random cases, and random cases are higher than serial cases. And the equivalent thermal conductivity increases with the increase of dry density.

The simulation evaluated the equivalent thermal conductivity fiber length in 6.35 mm (1/4 in.), 12.7 mm (1/2 in.), and 25.4 mm (1 in.). For the fiber distribution of random and parallel cases, the longer fiber length led to a higher equivalent thermal conductivity. For the evaluation of a single fiber case, the fiber-bentonite mixture has a higher equivalent thermal conductivity when the fibers are connected. Longer fibers can be observed as joining together shorter fibers, such as the fiber in the length of 1 in. can be seen as two 1/2-inch-long fibers joined together, or four 1/4-inch-long fibers joined together. An equivalent

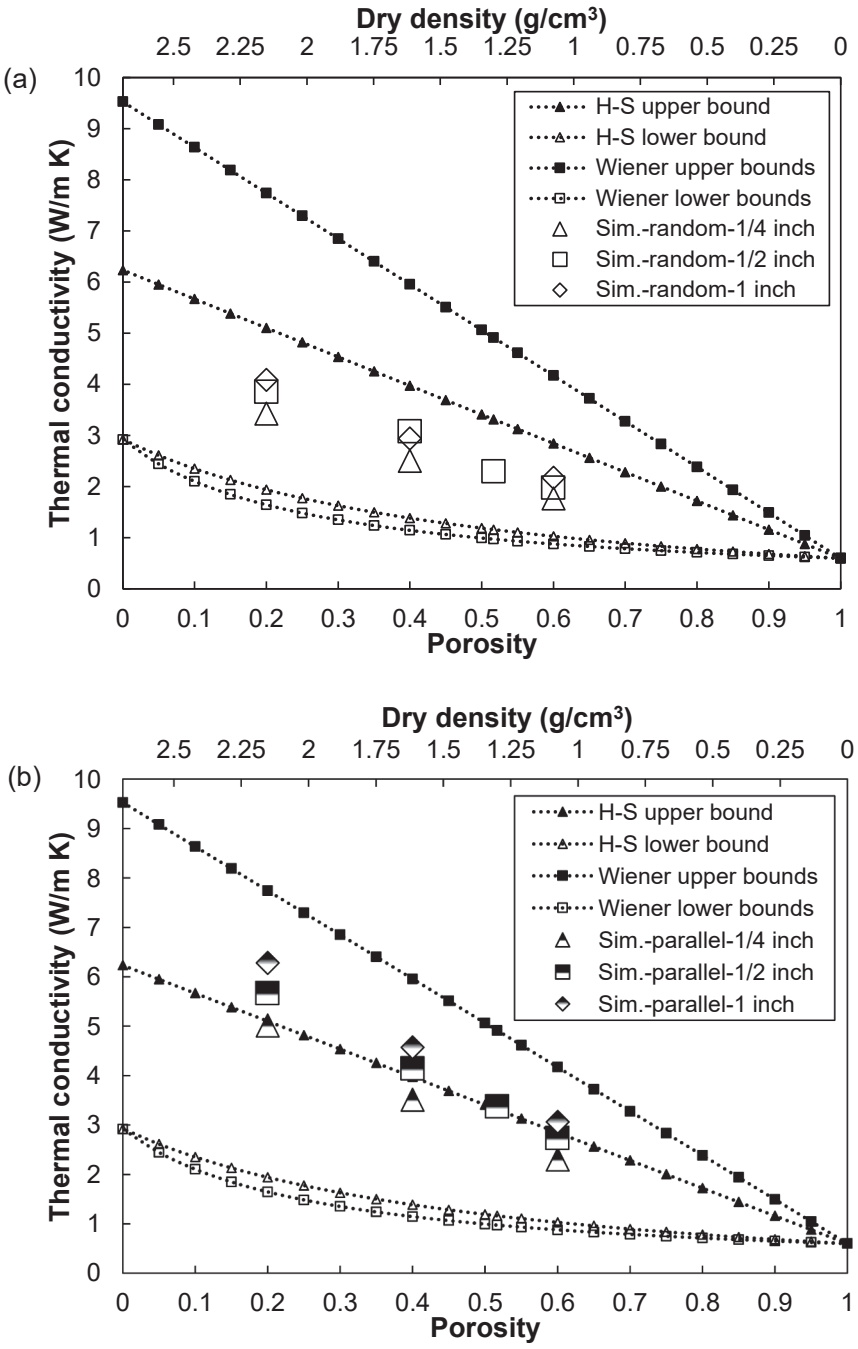

Fig. 11. Comparison of the equivalent thermal conductivity for H-S bounds, Wiener bounds, and FEM simulation results with different fiber lengths: 1 in., 0.5 in., and 0.25 in.; fiber content is 1 % by gravity; carbon fiber thermal conductivity is 1000 W/(m K). (a) random distribution, (b) parallel distribution, (c) serial distribution.

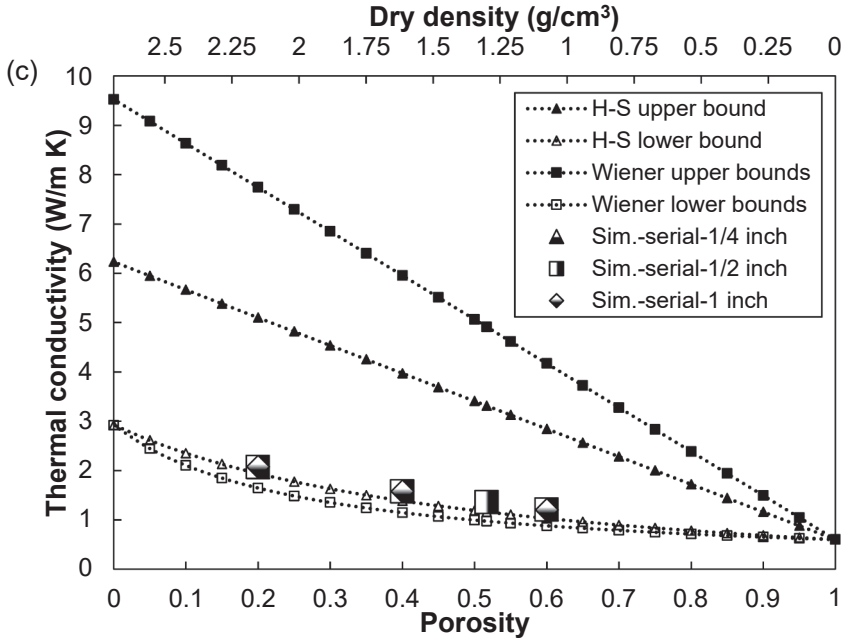

Fig. 11. (*continued*).

thermal conductivity difference caused by the fiber length is more significant in the case of the fiber distribution in parallel because the fiber orientation is close to the heat flux direction, which can facilitate heat transport. Similarly, the increase in dry density can also enhance the difference in equivalent thermal conductivity caused by the difference in fiber length. In the case of fiber distribution in serial, the change of the fiber length did not bring about significant changes in the equivalent thermal conductivity because the bentonite dominated it, which agreed with the single fiber case analysis.

Fig. 12 shows the contour of heat flux in bentonite with a fiber distribution in random, parallel, and serial. For randomly distributed fibers, the heat flux in the bentonite isolated by carbon fibers is relatively small because the heat is conducted by the carbon fibers with a much higher thermal conductivity than bentonite. The heat flux in the bentonite between the carbon fiber ends is relatively large because the bentonite mainly conducts the heat in this part of the area. As well for parallel and serial cases, the heat flux in bentonite between carbon fibers is relatively lower than near the end of the fibers. While in the case of series distribution of fiber, the heat flux difference inside the bentonite is slight, mainly concentrated in the range of 150 to 170 W/m^2. This is because although carbon fiber has a high thermal conductivity, it is isolated by bentonite and cannot effectively enhance heat transfer. Moreover, the average heat flux of bentonite for the three cases of random, parallel, and serial is 162.25 W/m^2, 175.23 W/m^2, and 157.03 W/m^2, respectively. The heat transport rate in bentonite is different because of the different enhancement effects of the distribution of different fibers, which agree with the equivalent thermal conductivity differences.

In addition to the heat flux within the bentonite, Fig. 13 shows the heat conduction flux in two intersecting fibers and the bentonite between them. The heat flux in the bentonite is tracked through the path, as shown in Fig. 13(a). Obviously, the heat flux in carbon fibers is significantly higher than that of bentonite near them, and there is a more than 100 times difference. The heat flux at the ends of the fibers is slightly lower than in the middle, while the opposite is true for bentonite. Also, there is a jump of the heat flux at the intersecting point because there is a heat exchange between the two fibers. It was assumed that the intersecting fibers have perfect contact in the simulation, but this differs from reality, which needs more discussion in future research (Wen et al., 2022b). The average heat flux in fibers in the random, parallel, and serial distribution is 19348 W/m^2, parallel, 65182 W/m^2, and serial, 3099 W/m^2, respectively. For the overall mixture, the more fibers in the same direction as the heat conduction intersecting with each other, the more conducive to heat conduction. Fibers that form a network in the direction of heat conduction can act as efficient pathways for heat conduction. This means the carbon fibers are more effective in enhancing heat transport in the case of distribution of parallel. However, in reality, the fibers may be in direct contact, or the contact points are filled by bentonite, and the heat transfer efficiency may be reduced when the contact between the fibers is poor, which can cause some overestimated results in the simulation.

Fig. 14 shows the equivalent thermal conductivity changes with fiber content in the case of the fiber distribution is random. The equivalent thermal conductivity increases with the fiber content. On the other hand, the fiber length in the higher fiber content gives a more substantial influence. The higher fiber content means an increase in the volume content of the fiber. From analyzing a single fiber, a high fiber content brings a high equivalent thermal conductivity. According to previous studies, the research on the thermal management of carbon nanotube composites indicated that forming a fiber network helps improve the equivalent thermal conductivity (Biercuk et al., 2002). The increase in the number of fibers means that the probability of fibers contacting each other increases to form a network.

In the above discussion, the numerical results of the thermal conductivity of carbon fiber reinforced bentonite range between maximum and minimum estimated from theoretical models, mainly because the two models did not consider the large aspect ratio of fibers. When constructing a theoretical model of a fiber mixture, more factors might be considered besides the ratio of the components, such as fiber aspect ratio, fiber and soil particles, the contact thermal resistance between components, the distribution of fibers, the bending of fibers, etc.

4.4. Summary of simulation results

The simulation results of all the cases as shown in Fig. 15. Fiber distribution in parallel, longer fiber length, higher fiber content, and higher dry density of bentonite are conducive to the improvement of equivalent thermal conductivity. In the serial cases, the enhancement brought about by fiber length and fiber content is very weak. Only a slight improvement is brought about by the increase in the dry density of

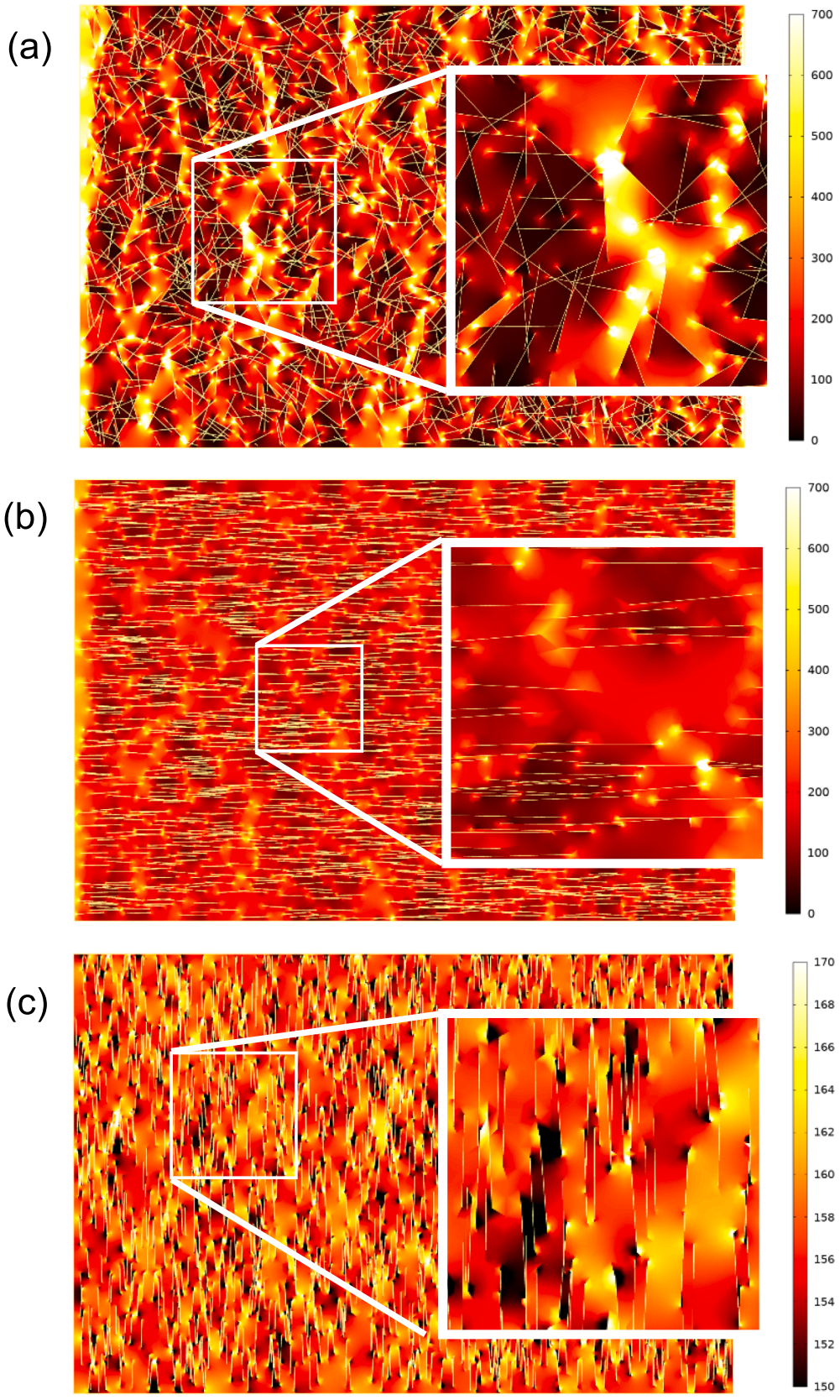

Fig. 12. The contour of heat flux (W/m^2) of carbon fiber reinforced bentonite with different fiber distributions, fiber content: 1.0 %, bentonite porosity: 0.4; fiber length: 12.7 mm; carbon fiber thermal conductivity: 1000 W/(m K); heat transport from right to left with a temperature difference of 30 K. (a) random, (b) parallel, (c) serial.

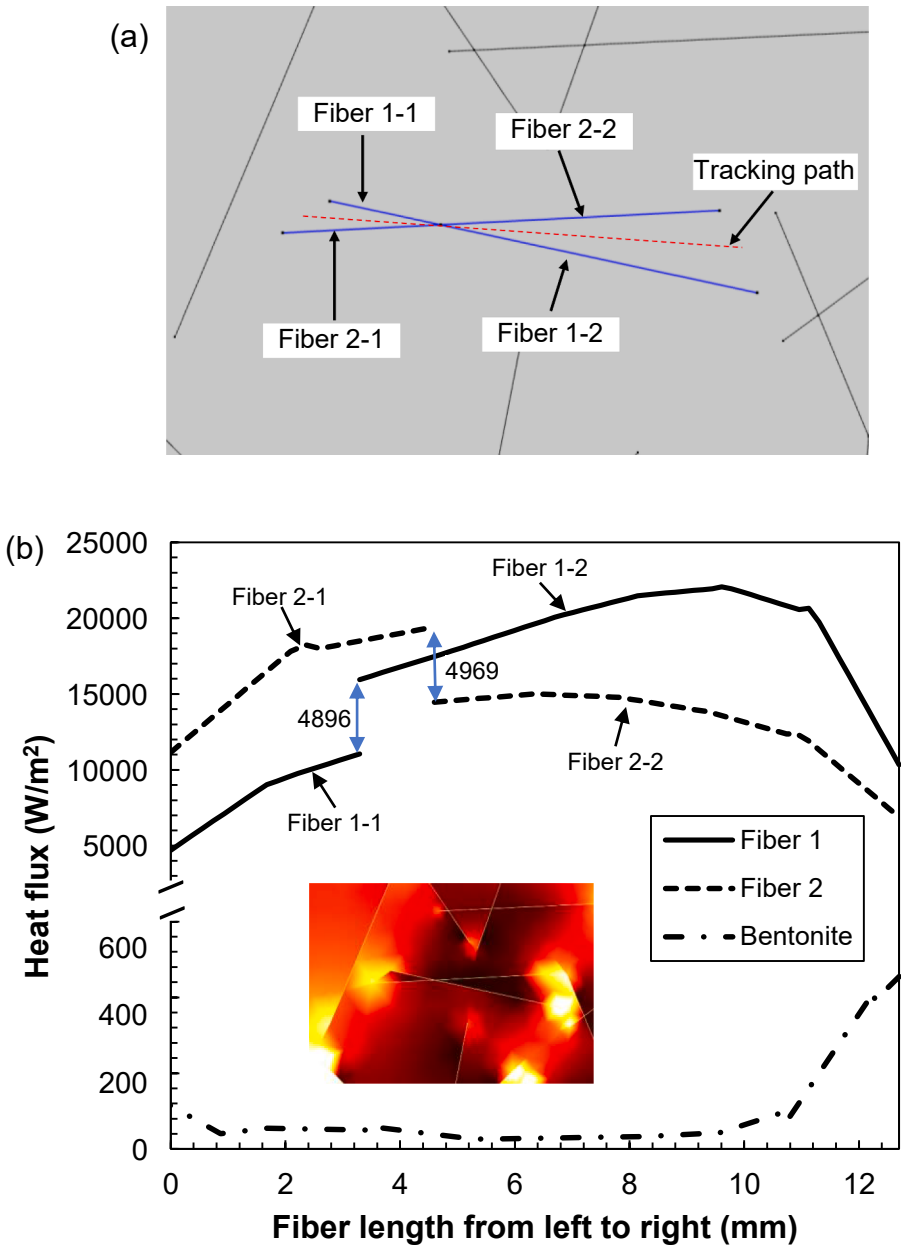

Fig. 13. Heat flux inside two intersecting fibers, a random distribution of fiber with a length of 12.7 mm and a diameter of 0.01 mm, fiber content is 1.0 %, (a) Two intersecting fibers in the simulation model with the fiber distribution of random, (b) heat flux in the two fibers and the bentonite between them.

bentonite. The enhancement brought about by higher fiber content and longer fiber length is more pronounced at higher dry density and distribution in parallel.

As mentioned above, the higher thermal conductivity of carbon fiber would effectively be pronounced by the improvement brought about by increasing fiber content, distribution, and fiber length. The effectiveness of carbon fiber with a higher thermal conductivity is worth investigating. At the same time, the bending of fibers is also an obstacle to forming fiber networks. Fibers with a large aspect ratio (longer fiber) are easier to form a network if the fibers are straight, but a larger aspect ratio is easier to bend in mixing. It is very meaningful to choose the fiber with the optimal aspect ratio in the application (Agari et al., 1993; Burger et al., 2016; Qureshi et al., 2018).

In addition, the contact conditions between fibers and between fibers and bentonite are important for heat conduction. In this study, the bentonite is in a saturated state, and fibers are in good contact with bentonite, and the thermal resistance between fibers and bentonite is neglected (Hasselman et al., 1993; Pal, R. 2005). However, for unsaturated bentonite or dried bentonite, there may be air between the fiber and bentonite, the thermal conductivity of air is significantly lower than that of bentonite particles and fibers, and the contact thermal resistance cannot be neglected. Likewise, the thermal contact resistance between fibers is also of concern, especially when the voids between fibers in a fiber cluster are filled with air.

As mentioned above, the bentonite in this study is in a saturated state; however, the environment in which the bentonite is used will cause changes in moisture content and affect thermal conductivity. On the one hand, decreasing moisture content will replace the water in the voids with the air of lower thermal conductivity, which reduces the thermal conductivity of the material (Kim et al., 2015; Lee et al., 2016; Xu et al., 2019). On the other hand, bentonite is the characteristic of shrinking after dehydration, and drying cracks will aggravate the decrease of thermal conductivity. Although adding fibers inhibits crack development, some microcracks cannot be avoided (Kawaragi et al.,

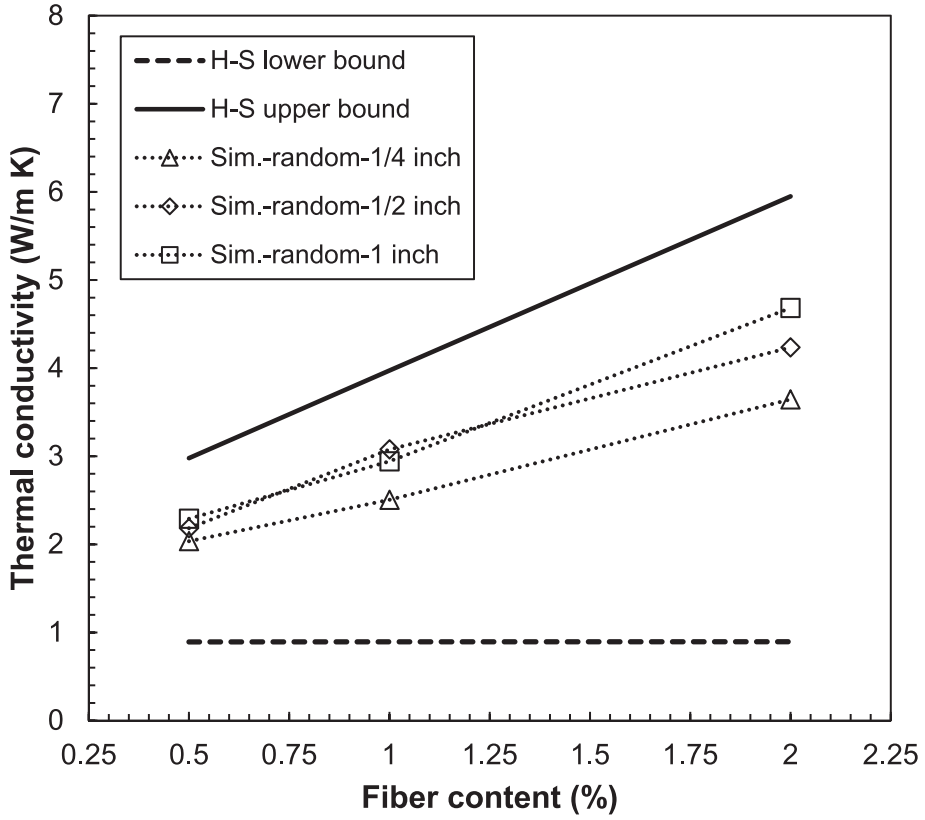

Fig. 14. Comparison of the equivalent thermal conductivity for H-S bounds and FEM simulation results with different fiber lengths: 1 in., 0.5 in., and 0.25 in.; fiber is randomly distributed; fiber contents are 0.5 %, 1 %, and 2 % by gravity; carbon fiber thermal conductivity is 1000 W/(m K); dry density is 1.61 g/cm^3.

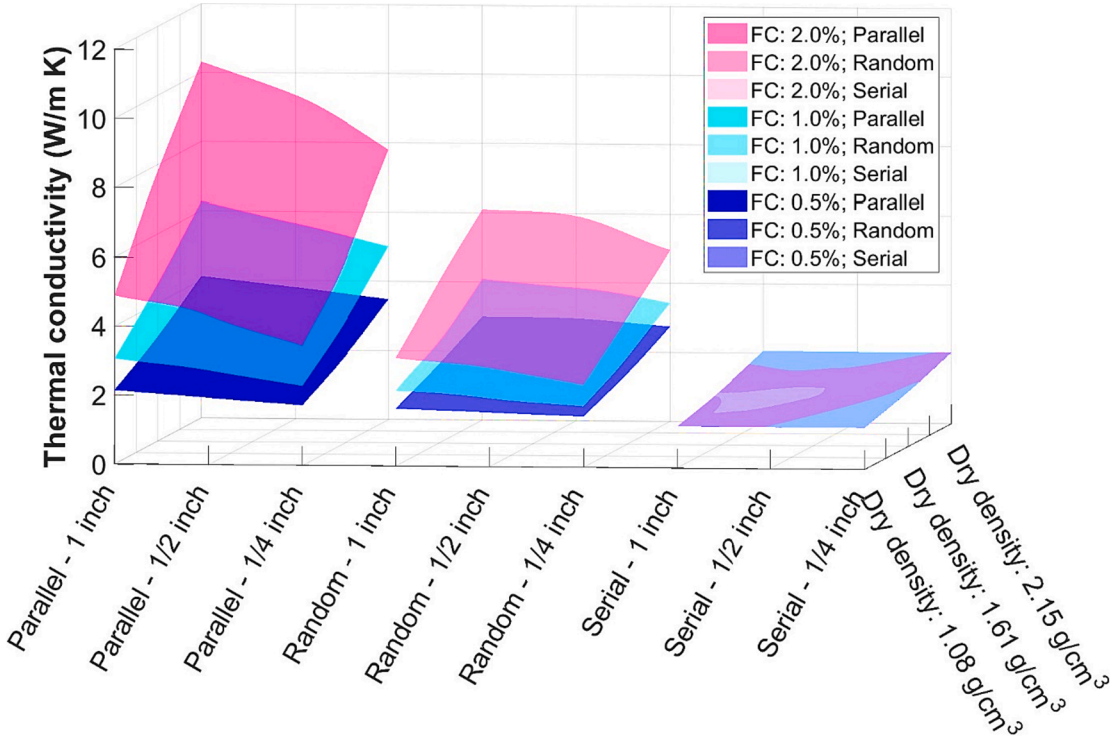

Fig. 15. The effects of dry density, fiber content (FC), fiber length, and fiber distribution on the thermal conductivity of fiber-reinforced bentonite from simulation. Dry density: 1.08, 1.61, and 2.15 g/cm^3; FC: 0.5 %, 1.0 %, and 2.0 %; fiber length: 1/4 in., 1/2 in., and 1.0 in.; carbon fiber thermal conductivity is 1000 W/(m K); fiber distribution: parallel, random, and serial.

2009; Zhang et al., 2017; Taheri & El-Zein, 2023). Moreover, desiccation would reduce the contact area between carbon fiber and bentonite particles, increasing the contact thermal resistance, which would greatly reduce the enhancement effect of carbon fiber on thermal conductivity. In addition, the interaction between bentonite and carbon fiber may affect the contact situation, which may also be a factor affecting crack behavior, mechanical stability, and thermal conductivity (Wang et al. 2016; Liu et al., 2019; Ruan et al., 2022; Calaunan et al., 2023). Future research will discuss the effect of different initial moisture content and desiccation on the thermal conductivity of carbon fiber-reinforced bentonite, which will help to find a suitable initial state of the material for engineering applications.

5. Conclusions

A series of simulations and laboratory experiments were conducted to determine the equivalent thermal conductivity of carbon fiber-reinforced bentonite. The resulting multiphase mixture of carbon fiber-reinforced bentonite, which consists of air, fibers, water, and bentonite particles, was evaluated through FEM simulations to analyze the effects of fiber content, distribution, length, and dry density on the equivalent thermal conductivity. Additionally, an analytical solution and simulation were conducted for a single fiber case to examine the impact of fiber spacing on the equivalent thermal conductivity. Overall, the research findings demonstrate the potential for using carbon fiber to enhance the thermal conductivity and stability of bentonite in heat-sensitive engineering applications. The main conclusions are:

1. When the fiber content is fixed, the equivalent thermal conductivity increases with the increase of the spacing in the case of the fiber distribution parallel to the heat flux direction, and the equivalent thermal conductivity changes little with the increase of the spacing when the fiber distribution is serial.
2. The equivalent thermal conductivity obtained from the simulation falls within H-S bounds. Parallel case falls around the upper bound and serial case falls near the lower bound, and random case in the middle. The equivalent thermal conductivity may be greater than the H-S upper bound for longer fibers and larger dry densities. When the fiber content is 1.0 %, the length is greater than 12.7 mm (0.5 in.), and the dry density is greater than 1.61 g/cm^3, the equivalent thermal conductivity is greater than the H-S upper bound but lower than the Wiener upper bound.
3. The increase in dry density of bentonite and fiber content significantly enhances equivalent thermal conductivity. When the content of carbon fiber with a thermal conductivity of 1000 W/(m K) is 1.0 %, and the porosity of bentonite is 0.4, the thermal conductivity of the composite can be increased by up to 390 % compared to pure bentonite.
4. The increase in fiber length will give different enhancements under different fiber content and dry density of bentonite. The thermal conductivity of the mixture for 1-inch fibers is 1.11 and 1.29 times that of 1/2-inch and 1/4-inch fibers. At the same time, the distribution of fibers plays a vital role in thermal conductivity, and the thermal conductivity in the case of parallel distribution is 1.48 and 2.91 times that of random distribution and serial distribution.
5. The heat flux in carbon fiber is higher than that of bentonite, which can reach two orders of magnitude higher. It is more conducive to heat conduction when the heat flux direction is consistent with the fiber direction.
6. Following this study, it is worth investigating additional factors that influence the thermal conductivities, such as fiber clusters, bending and uneven distribution of fibers, bentonite saturation, and drying shrinkage. Moreover, when considering the extreme environmental conditions in the application, various factors need to be taken into account, including water content variation, drying and wetting cycles, temperature fluctuations affecting the thermal conductivity of bentonite-fiber mixtures, THM coupled properties, and so on.

CRediT authorship contribution statement

Yuan Feng: Investigation, Data curation, Validation, Writing – original draft. **Jongwan Eun:** Conceptualization, Methodology, Funding acquisition, Supervision, Writing – review & editing. **Seunghee Kim:** Conceptualization, Writing – review & editing. **Yong-Rak Kim:** Conceptualization, Writing – review & editing.

Declaration of Competing Interest

The authors declare that they have no known competing financial interests or personal relationships that could have appeared to influence the work reported in this paper.

Data availability

Data will be made available on request.

Acknowledgment

The authors appreciate the financial support from the Nuclear Energy University Programs (NEUP) (Grant ID: DE-NE0008954) of the Department of Energy (DOE) and the finding and conclusions do not necessarily reflect the sponsor's perspectives.

References

Abu-Hamdeh, N.H., 2001. SW—Soil and water: measurement of the thermal conductivity of sandy loam and clay loam soils using single and dual probes. J. Agric. Eng. Res. 80 (2), 209–216. https://doi.org/10.1006/jaer.2001.0730.

Agari, Y., Ueda, A., Nagai, S., 1993. Thermal conductivity of a polymer composite. J. Appl. Polym. Sci. 49 (9), 1625–1634. https://doi.org/10.1002/app.1993.070490914.

Akbari, A., Akbari, M., Hill, R.J., 2013. Effective thermal conductivity of two-dimensional anisotropic two-phase media. Int. J. Heat Mass Transf. 63, 41–50. https://doi.org/10.1016/j.ijheatmasstransfer.2013.03.008.

Allan, M.L., Kavanaugh, S.P., 1999. Thermal conductivity of cementitious grouts and impact on heat exchanger length design for ground source heat pumps. Hvac&R Research 5 (2), 85–96. https://doi.org/10.1080/10789669.1999.10391226.

Behzad, T., Sain, M., 2007. Measurement and prediction of thermal conductivity for hemp fiber reinforced composites. Polym. Eng. Sci. 47 (7), 977–983. https://doi.org/10.1002/pen.20632.

Bekhiti, M., Trouzine, H., Rabehi, M., 2019. Influence of waste tire rubber fibers on swelling behavior, unconfined compressive strength and ductility of cement stabilized bentonite clay soil. Constr. Build. Mater. 208, 304–313. https://doi.org/10.1016/j.conbuildmat.2019.03.011.

Beswick, A.J., Gibb, F.G., Travis, K.P., 2014. Deep borehole disposal of nuclear waste: engineering challenges. Proceedings of the Institution of Civil Engineers-Energy 167 (2), 47–66. https://doi.org/10.1680/ener.13.00016.

Biercuk, M.J., Llaguno, M.C., Radosavljevic, M., Hyun, J.K., Johnson, A.T., Fischer, J.E., 2002. Carbon nanotube composites for thermal management. Appl. Phys. Lett. 80 (15), 2767–2769. https://doi.org/10.1063/1.1469696.

Bojnourdi, S., Narani, S.S., Abbaspour, M., Ebadi, T., Hosseini, S.M.M., 2020. Hydro-mechanical properties of unreinforced and fiber-reinforced used motor oil (UMO)-contaminated sand-bentonite mixtures. Eng. Geol. 279, 105886 https://doi.org/10.1016/j.enggeo.2020.105886.

Brahmachary, T.K., Rokonuzzaman, M., 2018. Investigation of random inclusion of bamboo fiber on ordinary soil and its effect CBR value. Int. J. Geo-Eng. 9, 1–11. https://doi.org/10.1186/s40703-018-0079-x.

Bristow, K.L., White, R.D., Kluitenberg, G.J., 1994. Comparison of single and dual probes for measuring soil thermal properties with transient heating. Soil Res. 32 (3), 447–464. https://doi.org/10.1071/SR9940447.

Burger, N., Laachachi, A., Ferriol, M., Lutz, M., Toniazzo, V., Ruch, D., 2016. Review of thermal conductivity in composites: Mechanisms, parameters and theory. Prog. Polym. Sci. 61, 1–28. https://doi.org/10.1016/j.progpolymsci.2016.05.001.

Calaunan, Jose Maria Ferdinand, Feng, Yuan, Eun, Jongwan, Kim, Seunghee, and Yong-Rak Kim. "Evaluation of Shearing Behavior of Inorganic Microfiber-Reinforced Bentonite for Engineered Barrier Materials." *Paper presented at the 57th U.S. Rock Mechanics/Geomechanics Symposium*, Atlanta, Georgia, USA, June 2023. https://doi.org/10.56952/ARMA-2023-0880.

Carson, J.K., Lovatt, S.J., Tanner, D.J., Cleland, A.C., 2005. Thermal conductivity bounds for isotropic, porous materials. Int. J. Heat Mass Transf. 48 (11), 2150–2158. https://doi.org/10.1016/S0017-9310(05)00067-0.

Chen, J.N., Benson, C.H., Edil, T.B., 2018. Hydraulic conductivity of geosynthetic clay liners with sodium bentonite to coal combustion product leachates. J. Geotech. Geoenviron. Eng. 144 (3), 04018008. https://doi.org/10.1061/(ASCE)GT.1943-5606.0001844.

Chen, H., Ginzburg, V.V., Yang, J., Yang, Y., Liu, W., Huang, Y., Chen, B., 2016. Thermal conductivity of polymer-based composites: Fundamentals and applications. Prog. Polym. Sci. 59, 41–85. https://doi.org/10.1016/j.progpolymsci.2016.03.001.

Delaleux, F., Py, X., Olives, R., Dominguez, A., 2012. Enhancement of geothermal borehole heat exchangers performances by improvement of bentonite grouts conductivity. Appl. Therm. Eng. 33, 92–99. https://doi.org/10.1016/j.applthermaleng.2011.09.017.

Deng, F., Zheng, Q.S., Wang, L.F., Nan, C.W., 2007. Effects of anisotropy, aspect ratio, and nonstraightness of carbon nanotubes on thermal conductivity of carbon nanotube composites. Appl. Phys. Lett. 90 (2), 021914 https://doi.org/10.1063/1.2430914.

Di Sipio, E., Bertermann, D., 2018. Thermal properties variations in unconsolidated material for very shallow geothermal application (ITER project). Int. Agrophys. 32 (2) https://doi.org/10.1515/intag-2017-0002.

Dong, Y., McCartney, J.S., Lu, N., 2015. Critical review of thermal conductivity models for unsaturated soils. Geotech. Geol. Eng. 33 (2), 207–221. https://doi.org/10.1007/s10706-015-9843-2.

Eisenhour, D.D., Brown, R.K., 2009. Bentonite and its impact on modern life. Elements 5 (2), 83–88. https://doi.org/10.2113/gselements.5.2.83.

Ewing, R.P., Horton, R., 2007. Thermal conductivity of a cubic lattice of spheres with capillary bridges. J. Phys. D Appl. Phys. 40 (16), 4959. https://doi.org/10.1088/0022-3727/40/16/031.

Feng, Y., Eun, J., Kim, S., Kim, Y.R., 2021. Comparison of desiccation cracks between bentonite and inorganic microfiber reinforced bentonite for engineered barrier system. Trans. Am. Nucl. Soc. 124 (1), 125–127. https://doi.org/10.13182/T124-35616.

Finsterle, S., Muller, R.A., Baltzer, R., Payer, J., Rector, J.W., 2019. Thermal evolution near heat-generating nuclear waste canisters disposed in horizontal drillholes. Energies 12 (4), 596. https://doi.org/10.3390/en12040596.

Fu, S.Y., Mai, Y.W., 2003. Thermal conductivity of misaligned short-fiber-reinforced polymer composites. J. Appl. Polym. Sci. 88 (6), 1497–1505. https://doi.org/10.1002/app.11864.

Fujii, M., Zhang, X., Xie, H., Ago, H., Takahashi, K., Ikuta, T., Shimizu, T., 2005. Measuring the thermal conductivity of a single carbon nanotube. Phys. Rev. Lett. 95 (6), 065502 https://doi.org/10.1103/PhysRevLett.95.065502.

Gao, H., Zhang, L., Zhang, D., Ji, T., Song, J., 2021. Mechanical properties of fiber-reinforced asphalt concrete: Finite element simulation and experimental study. E-Polymers 21 (1), 533–548. https://doi.org/10.1515/epoly-2021-0057.

Guzman, I.L., Payano, C., 2023. Use of repurposed whole textile for enhancement of pavement soils. Int. J. Geo-Eng. 14, 12. https://doi.org/10.1186/s40703-023-00190-1.

Hamilton, R.L., Crosser, O.K., 1962. Thermal conductivity of heterogeneous two-component systems. Ind. Eng. Chem. Fundam. 1 (3), 187–191. https://doi.org/10.1021/i160003a005.

Hasselman, D.P.H., Donaldson, K.Y., Thomas Jr, J.R., 1993. Effective thermal conductivity of uniaxial composite with cylindrically orthotropic carbon fibers and interfacial thermal barrier. J. Compos. Mater. 27 (6), 637–644. https://doi.org/10.1177/002199839302700605.

Haynes, H.M., Bailey, M.T., Lloyd, J.R., 2021. Bentonite barrier materials and the control of microbial processes: Safety case implications for the geological disposal of radioactive waste. Chem. Geol. 581, 120353 https://doi.org/10.1016/j.chemgeo.2021.120353.

Javanbakht, Z., Hall, W., Öchsner, A., 2019. Effective thermal conductivity of fiber reinforced composites under orientation clustering. Engineering design applications 507–519. https://doi.org/10.1007/978-3-319-79005-3_32.

Kale, R.C., Ravi, K., 2021. A review on the impact of thermal history on compacted bentonite in the context of nuclear waste management. Environ. Technol. Innov. 23, 101728 https://doi.org/10.1016/j.eti.2021.101728.

Katsumi, T., Ishimori, H., Onikata, M., Fukagawa, R., 2008. Long-term barrier performance of modified bentonite materials against sodium and calcium permeant solutions. Geotext. Geomembr. 26 (1), 14–30. https://doi.org/10.1016/j.geotexmem.2007.04.003.

Kawaragi, C., Yoneda, T., Sato, T., Kaneko, K., 2009. Microstructure of saturated bentonites characterized by X-ray CT observations. Eng. Geol. 106 (1–2), 51–57. https://doi.org/10.1016/j.enggeo.2009.02.013.

Kim, D., Kim, G., Baek, H., 2015. Relationship between thermal conductivity and soil–water characteristic curve of pure bentonite-based grout. Int. J. Heat Mass Transf. 84, 1049–1055. https://doi.org/10.1016/j.ijheatmasstransfer.2015.01.091.

Kim, D., Kim, G., Baek, H., 2015. Relationship between thermal conductivity and soil–water characteristic curve of pure bentonite-based grout. Int. J. Heat Mass Transf. 84, 1049–1055. https://doi.org/10.1016/j.ijheatmasstransfer.2015.01.091.

Kodicherla, S.P.K., Nandyala, D.K., 2019. Influence of randomly mixed coir fibres and fly ash on stabilization of clayey subgrade. Int. J. Geo-Eng. 10 (1), 3. https://doi.org/10.1186/s40703-019-0099-1.

Kumanek, B., Janas, D., 2019. Thermal conductivity of carbon nanotube networks: A review. J. Mater. Sci. 54 (10), 7397–7427. https://doi.org/10.1007/s10853-019-03368-0.

Lee, J.O., Choi, H., Lee, J.Y., 2016. Thermal conductivity of compacted bentonite as a buffer material for a high-level radioactive waste repository. Ann. Nucl. Energy 94, 848–855. https://doi.org/10.1016/j.anucene.2016.04.053.

Lee, C., Lee, K., Choi, H., Choi, H.P., 2010. Characteristics of thermally-enhanced bentonite grouts for geothermal heat exchanger in South Korea. Sci. China Ser. E: Technol. Sci. 53 (1), 123–128. https://doi.org/10.1007/s11431-009-0413-9.

Lee, G.J., Yoon, S., Cho, W.J., 2021. Effect of bentonite type on thermal conductivity in a HLW repository. Journal of Nuclear Fuel Cycle and Waste Technology 19 (3), 331–338. https://doi.org/10.7733/jnfcwt.2021.19.3.331.

Levasseur, S., Sillen, X., Marschall, P., Wendling, J., Olin, M., Grgic, D., Svoboda, J., 2022. EURADWASTE'22 Paper-Host rocks and THMC processes in DGR. EURAD GAS and HITEC: mechanistic understanding of gas and heat transport in clay-based materials for radioactive waste geological disposal. EPJ N-Nuclear Sciences & Technologies 8. https://doi.org/10.1051/epjn/2022021.

Likos, W.J., 2015. Pore-scale model for thermal conductivity of unsaturated sand. Geotech. Geol. Eng. 33 (2), 179–192. https://doi.org/10.1007/s10706-014-9744-9.

Liu, L., Cai, G., Liu, X., Liu, S., Puppala, A.J., 2019. Evaluation of thermal-mechanical properties of quartz sand–bentonite–carbon fiber mixtures as the borehole backfilling material in ground source heat pump. Energ. Buildings 202, 109407. https://doi.org/10.1016/j.enbuild.2019.109407.

Liu, K., Lu, L., Wang, F., Liang, W., 2017. Theoretical and experimental study on multi-phase model of thermal conductivity for fiber reinforced concrete. Constr. Build. Mater. 148, 465–475. https://doi.org/10.1016/j.conbuildmat.2017.05.043.

Liu, L. (2007). Hashin-shtrikman bounds for multiphase composites and their attainability, *Proceedings of the Royal Society A: Mathematical, Physical and Engineering Science, To Appear*. Doi: 10.1098/rspa.2009.0554.

Lu, Y., Lu, S., Horton, R., Ren, T., 2014. An empirical model for estimating soil thermal conductivity from texture, water content, and bulk density. Soil Sci. Soc. Am. J. 78 (6), 1859–1868. https://doi.org/10.2136/sssaj2014.05.0218.

Lu, Z., Yuan, Z., Liu, Q., Hu, Z., Xie, F., Zhu, M., 2015. Multi-scale simulation of the tensile properties of fiber-reinforced silica aerogel composites. Mater. Sci. Eng. A 625, 278–287. https://doi.org/10.1016/j.msea.2014.12.007.

Macias, J.D., Bante-Guerra, J., Cervantes-Alvarez, F., Rodrìguez-Gattorno, G., Arés-Muzio, O., Romero-Paredes, H., Alvarado-Gil, J.J., 2019. Thermal characterization of carbon fiber-reinforced carbon composites. Appl. Compos. Mater. 26, 321–337. https://doi.org/10.1007/s10443-018-9694-0.

Montes-H, G., Geraud, Y., 2004. Sorption kinetic of water vapour of MX80 bentonite submitted to different physical–chemical and mechanical conditions. Colloids Surf A Physicochem Eng Asp 235 (1–3), 17–23. https://doi.org/10.1016/j.colsurfa.2004.01.013.

Nikoosokhan, S., Nowamooz, H., Chazallon, C., 2016. Effect of dry density, soil texture and time-spatial variable water content on the soil thermal conductivity. Geomech. Geoeng. 11 (2), 149–158. https://doi.org/10.1080/17486025.2015.1048313.

Orakoglu, M.E., Liu, J., Niu, F., 2016. Experimental and modeling investigation of the thermal conductivity of fiber-reinforced soil subjected to freeze-thaw cycles. Appl. Therm. Eng. 108, 824–832. https://doi.org/10.1016/j.applthermaleng.2016.07.112.

Pal, R., 2005. Porosity-dependence of effective mechanical properties of pore-solid composite materials. J. Compos. Mater. 39 (13), 1147–1158. https://doi.org/10.1177/0021998305048744.

Phan-Thien, N., Milton, G.W., 1982. New bounds on the effective thermal conductivity of N-phase materials. *Proc. R. Soc. Lond.* A. Mathematical and Physical Sciences 380 (1779), 333–348. https://doi.org/10.1098/rspa.1982.0045.

Pietrak, K., Wiśniewski, T.S., 2015. A review of models for effective thermal conductivity of composite materials. Journal of Power Technologies 95 (1). https://doi.org/10.1016/j.jpowtec.2014.12.012.

Qureshi, Z.A., Ali, H.M., Khushnood, S., 2018. Recent advances on thermal conductivity enhancement of phase change materials for energy storage system: a review. Int. J. Heat Mass Transf. 127, 838–856. https://doi.org/10.1016/j.ijheatmasstransfer.2018.08.049.

Ravi, K., Rao, S.M., 2013. Influence of infiltration of sodium chloride solutions on SWCC of compacted bentonite–sand specimens. Geotech. Geol. Eng. 31, 1291–1303. https://doi.org/10.1007/s10706-013-9650-6.

Ruan, K., Wang, H., Komine, H., Ito, D., 2022. Experimental study for temperature effect on swelling pressures during saturation of bentonites. Soils Found. 62 (6), 101245 https://doi.org/10.1016/j.sandf.2022.101245.

Scalia IV, J., Benson, C.H., Bohnhoff, G.L., Edil, T.B., Shackelford, C.D., 2014. Long-term hydraulic conductivity of a bentonite-polymer composite permeated with aggressive inorganic solutions. J. Geotech. Geoenviron. Eng. 140 (3), 04013025. https://doi.org/10.1061/(ASCE)GT.1943-5606.0001040.

Scalia IV, J., Bohnhoff, G.L., Shackelford, C.D., Benson, C.H., Sample-Lord, K.M., Malusis, M.A., Likos, W.J., 2018. Enhanced bentonites for containment of inorganic waste leachates by GCLs. Geosynth. Int. 25 (4), 392–411. https://doi.org/10.1680/jgein.18.00024.

Shim, H.B., Seo, M.K., Park, S.J., 2002. Thermal conductivity and mechanical properties of various cross-section types carbon fiber-reinforced composites. J. Mater. Sci. 37 (9), 1881–1885. https://doi.org/10.1023/A:1014959603892.

Sun, X., Gao, Z., Cao, P., Zhou, C., 2019. Mechanical properties tests and multiscale numerical simulations for basalt fiber reinforced concrete. Constr. Build. Mater. 202, 58–72. https://doi.org/10.1016/j.conbuildmat.2019.01.018.

Sundberg J. 1988. Thermal properties of soils and rocks. Ph.D. Thesis, Department of Geoglogy, Chalmers University of Technology and University of Gothenburg, G. ooteborg, Sweden Publ. A57, 1–310.

Taheri, S., El-Zein, A., 2023. Desiccation cracking of polymer-bentonite mixtures: An experimental investigation. Appl. Clay Sci. 238, 106945 https://doi.org/10.1016/j.clay.2023.106945.

Tarnawski, V.R., Leong, W.H., Gori, F., Buchan, G.D., Sundberg, J., 2002. Inter-particle contact heat transfer in soil systems at moderate temperatures. Int. J. Energy Res. 26 (15), 1345–1358. https://doi.org/10.1002/er.853.

Tarnawski, V.R., Leong, W.H., 2012. A series-parallel model for estimating the thermal conductivity of unsaturated soils. Int. J. Thermophys. 33 (7), 1191–1218. https://doi.org/10.1007/s10765-012-1282-1.

Tay, Y.Y., Stewart, D.I., Cousens, T.W., 2001. Shrinkage and desiccation cracking in bentonite–sand landfill liners. Eng. Geol. 60 (1–4), 263–274. https://doi.org/10.1016/S0013-7952(00)00107-1.

Thyagaraj, T., Soujanya, D., 2017. Polypropylene fiber reinforced bentonite for waste containment barriers. Appl. Clay Sci. 142, 153–162. https://doi.org/10.1016/j.clay.2017.02.009.

Toé Casagrande, M.D., Coop, M.R., Consoli, N.C., 2006. Behavior of a fiber-reinforced bentonite at large shear displacements. J. Geotech. Geoenviron. Eng. 132 (11), 1505–1508. https://doi.org/10.1061/(ASCE)1090-0241(2006)132:11(1505).

Tong, F., Jing, L., Zimmerman, R.W., 2009. An effective thermal conductivity model of geological porous media for coupled thermo-hydro-mechanical systems with multiphase flow. International Journal of Rock Mechanics and Mining Sciences 46 (8), 1358–1369. https://doi.org/10.1016/j.ijrmms.2009.04.010.

Vail, M., Zhu, C., Tang, C.S., Anderson, L., Moroski, M., Montalbo-Lomboy, M.T., 2019. Desiccation cracking behavior of MICP-treated bentonite. Geosciences 9 (9), 385. https://doi.org/10.3390/geosciences9090385.

Wang, H., Cui, Y., Qi, C., 2013. Effects of sand–bentonite backfill materials on the thermal performance of borehole heat exchangers. Heat Transfer Eng. 34 (1), 37–44. https://doi.org/10.1080/01457632.2013.694771.

Wang, Y., Hadgu, T., 2020. Enhancement of thermal conductivity of bentonite buffer materials with copper wires/meshes for high-level radioactive waste disposal. Nucl. Technol. 206 (10), 1584–1592. https://doi.org/10.1080/00295450.2019.1704577.

Wang, M., He, J., Yu, J., Pan, N., 2007. Lattice Boltzmann modeling of the effective thermal conductivity for fibrous materials. Int. J. Therm. Sci. 46 (9), 848–855. https://doi.org/10.1016/j.ijthermalsci.2006.11.006.

Wang, M., Kang, Q., Pan, N., 2009. Thermal conductivity enhancement of carbon fiber composites. Appl. Therm. Eng. 29 (2–3), 418–421. https://doi.org/10.1016/j.applthermaleng.2008.03.004.

Wang, H., Lei, Y.P., Wang, J.S., Qin, Q.H., Xiao, Y., 2016a. Theoretical and computational modeling of clustering effect on effective thermal conductivity of cement composites filled with natural hemp fibers. J. Compos. Mater. 50 (11), 1509–1521. https://doi.org/10.1177/0021998315594482.

Wang, Q., Meng, Y., Su, W., Ye, W., Chen, Y., 2021. Cracking and sealing behavior of the compacted bentonite upon technological voids filling. Eng. Geol. 292, 106244 https://doi.org/10.1016/j.enggeo.2021.106244.

Wang, H., Qin, Q.H., Xiao, Y., 2016b. Special n-sided Voronoi fiber/matrix elements for clustering thermal effect in natural-hemp-fiber-filled cement composites. Int. J. Heat Mass Transf. 92, 228–235. https://doi.org/10.1016/j.ijheatmasstransfer.2015.08.093.

Wen, M., Tian, Y., Li, L., Wang, K., Wu, W., 2022a. An imperfect thermal contact problem for consolidation of bilayered saturated soil subjected to ramp-type heating. Int. J. Heat Mass Transf. 190, 122755 https://doi.org/10.1016/j.ijheatmasstransfer.2022.122755.

Wen, M., Tian, Y., Li, L., Qiu, X., Wang, K., Wu, W., Xu, M., 2022b. A general interfacial thermal contact model for consolidation of bilayered saturated soils considering thermo-osmosis effect. Int. J. Numer. Anal. Meth. Geomech. 46 (12), 2375–2397. https://doi.org/10.1002/nag.3411.

Wersin, P., Johnson, L.H., McKinley, I.G., 2007. Performance of the bentonite barrier at temperatures beyond 100 C: A critical review. Physics and Chemistry of the Earth, Parts A/B/C 32 (8–14), 780–788. https://doi.org/10.1016/j.pce.2006.02.051.

Wiener, O., 1912. Abhandl Math-Phys Kl Ko ̈nigl Sachsischen Ges 32, 509.

Xu, Y., Zeng, Z., Lv, H., 2019. Temperature dependence of apparent thermal conductivity of compacted bentonites as buffer material for high-level radioactive waste repository. Appl. Clay Sci. 174, 10–14. https://doi.org/10.1016/j.clay.2019.03.017.

Xu, Y., Zhou, X., Sun, D.A., Zeng, Z., 2022. Thermal properties of GMZ bentonite pellet mixtures subjected to different temperatures for high-level radioactive waste repository. Acta Geotech. 17 (3), 981–992. https://doi.org/10.1007/s11440-021-01244-3.

Yang, J., Wu, H., He, S., Wang, M., 2015. Prediction of thermal conductivity of fiber/aerogel composites for optimal thermal insulation. Journal of Porous Media 18 (10). https://doi.org/10.1615/JPorMedia.2015013550.

Yoon, S., Jeon, J.S., Kim, G.Y., Seong, J.H., Baik, M.H., 2019. Specific heat capacity model for compacted bentonite buffer materials. Ann. Nucl. Energy 125, 18–25. https://doi.org/10.1016/j.anucene.2018.10.045.

Yoon, S., Lee, D.H., Cho, W.J., Lee, C., Cho, D.K., 2022. Evaluation of water suction for compacted bentonite buffer under elevated temperature conditions. Journal of Nuclear Fuel Cycle and Waste Technology 20 (2), 185–192. https://doi.org/10.7733/jnfcwt.2022.015.

Zhai, S., Zhang, P., Xian, Y., Zeng, J., Shi, B., 2018. Effective thermal conductivity of polymer composites: Theoretical models and simulation models. Int. J. Heat Mass Transf. 117, 358–374. https://doi.org/10.1016/j.ijheatmasstransfer.2017.09.067.

Zhang, X.D., Chen, Y.G., Ye, W.M., Cui, Y.J., Deng, Y.F., Chen, B., 2017. Effect of salt concentration on desiccation cracking behavior of GMZ bentonite. Environ. Earth Sci. 76 (15), 1–10. https://doi.org/10.1007/s12665-017-6872-6.

Zhang, T., Deng, Y., Cui, Y., Lan, H., Zhang, F., Zhang, H., 2019. Porewater salinity effect on flocculation and desiccation cracking behaviour of kaolin and bentonite considering working condition. Eng. Geol. 251, 11–23. https://doi.org/10.1016/j.enggeo.2019.02.007.

Zhang, N., Wang, Z., 2017. Review of soil thermal conductivity and predictive models. Int. J. Therm. Sci. 117, 172–183. https://doi.org/10.1016/j.ijthermalsci.2017.03.013.

Zhang, N., Yu, X., Pradhan, A., Puppala, A.J., 2015. Thermal conductivity of quartz sands by thermo-time domain reflectometry probe and model prediction. J. Mater. Civ. Eng. 27 (12), 04015059. https://doi.org/10.1061/(ASCE)MT.1943-5533.0001332.

Zimmerman, R.W., 1989. Thermal conductivity of fluid-saturated rocks. J. Pet. Sci. Eng. 3 (3), 219–227. https://doi.org/10.1016/0920-4105(89)90019-3.